Arnold et al. – "Biomass burning influence on high latitude tropospheric ozone and reactive nitrogen in summer 2008: a multi-model analysis based on POLMIP simulations".

Response to Reviewer comments

We thank the two anonymous referees for their careful review of our manuscript. Here we respond to comments made by each reviewer in turn. Reviewer comments are given in italic text, and our response in normal text. We have shown in bold new text that we have added to the manuscript in response to the comments.

Anonymous Referee #1

My main concern is the use of O3/CO as a diagnostic for ozone production. Recent work (e.g. see Zhang et al. [2014]) advises against using this diagnostic with- out verifying the assumption of negligible CO loss. Could the authors do that prior to publication in ACP? That would provide a much stronger foundation for the remainder of the analysis.

In order to address this point, we have investigated the chemical loss rate of CO (due to CO+OH reaction) in the region of our analysis (latitude > 50N, 850-250 hPa) in the MOZART-4 model. This model has supplied output on chemical rates from the POLMIP simulation. We find that daily chemical loss rates of CO are small (average 1.9 ppbv/day), ranging between 1.5%-4.5%, and are also partly compensated by chemical production of CO from VOC oxidation (average 0.9 ppbv/day) at the same locations. We compared the chemical CO loss rate with the chemical production rate of ozone at each model grid-point in the specified region. This comparison demonstrates that the chemical loss of CO is negligible, and is substantially outweighed by the fractional photochemical production rate of ozone in these air masses. We believe that this analysis provides a sound basis for our assumption that the ozone/CO slopes are useful diagnostics of chemical ozone formation. We have included some text in the manuscript to summarise our justification for the use of ozone/CO slopes: **"Recent studies have highlighted the need for caution regarding the use of O_3/CO slopes to diagnose photochemical ozone production, particularly in remote regions, due to slopes being artificially increased by chemical loss of CO due to reaction with OH (e.g. Voulgarakis et al., 2011; Zhang et al., 2014). Chemical rate output from the MOZART-4 model shows that in the domain of our study (latitude 50N-90N, 850-250 hPa) the daily chemical loss rate of CO is small (average 1.9 ppbv/day), equivalent to 1.5%-4.5%. This loss is partly offset by chemical production of CO from VOC oxidation (average 0.9 ppbv/day), and daily fractional rates of chemical ozone production at the same locations are substantially larger (~5 - 45%). This analysis suggests that chemical CO loss is unlikely to have a significant effect on our calculated ozone/CO slopes."**

Pg: 24575, lines 12-13: Grammar issue here. Missing "in"

Corrected.

Pg:24584, lines 25 onward: This designation would still be problematic if there was CO loss in the plume.

We have addressed the issue of CO loss above, and in light of our diagnosis of negligible CO loss we retain this designation and discussion.

Pg: 24586, lines 7-9: The authors should describe a) the implementation of and rational

for the HO2 uptake in GEOS-Chem, and 2) how this implementation impacts the abundances of PAN and other species relevant to the paper.

Uptake of HO_2 is included in GEOS-Chem such that it is irreversibly lost through conversion to H_2O on aerosol, rather than forming H_2O_2. The motivation for this is that joint atmospheric observations of HO_2 and H_2O_2 from field studies suggest that HO_2 uptake by aerosols may not produce H_2O_2. It has been proposed that the conversion of HO_2 to H_2O can be catalyzed by transition metals in aqueous aerosols. This motivation and implementation of the process in GEOS-Chem has been described and implemented in the GEOS-Chem model (details in Mao et al., (2013)). We do not have a comparable simulation without this treatment of HO_2 uptake with which we can compare PAN and other NOy species for POLMIP. Results from the Mao et al., (2013) study showed that in simulations with the $HO_2 \rightarrow H_2O$ aerosol conversion included, HOx concentrations are reduced due to reduction in the re-formation of HOx via photolysis of H_2O_2 (a 12% reduction in mass-weighted global mean OH). This was shown to increase CO concentrations due to an increased CO lifetime, particularly in the extra-tropics. In addition, surface ozone concentrations decrease in general by 3–10 ppb over North America and Eurasia relative to a simulation without the $HO_2 \rightarrow H_2O$ uptake. We have added text to Section 2 to summarise these points: **"The GEOS-Chem model includes a parameterization for transition metal-catalysed formation of H_2O from aerosol uptake of HO_2, rather than formation of H_2O_2. This process is effectively an irreversible loss for HOx, and is motivated by the suggestion from field observations that HO_2 uptake to aerosol may not produce H_2O_2. This motivation and the implementation of this scheme are described by Mao et al., (2013). The same study showed that inclusion of this process reduces the mass-weighted global mean OH concentration by 12%, and substantially increases CO concentrations at high latitudes due to an increased CO lifetime. It was also shown to reduce surface ozone by 3-10 ppbv over North America and Eurasia."**

Pg: 24588: lines 19-22: The standard version of GEOS-Chem does not emit NOy with this partitioning. This indicates that the model used in the comparison should probably be better documented. Somewhere in the text should point to a reference for this version with a statement that the model is not a public release version.

We apologise, but the information provided on NOy partitioning does not in fact apply to the POLMIP GEOS-Chem simulations. For implementation of the FINN fire emissions, the emissions were speciated as NOx only, to be consistent with the other models. We have removed the information on modified emitted NOy partitioning from the manuscript.

Figure 5 and Figure 7: There seem to be excessive significant figures in this set of figures.

Agreed. We have reduced these to 3 significant figures, consistent with their presentation in the main text.

Anonymous Referee #2

- There is no mention of how photolysis is treated in the models. Certainly radiation-driven processes are important in the summer Arctic troposphere, and it would be good to describe how this is simulated in the models. Are "real-time" clouds, aerosols, surface albedos affecting the simulation? And how do factors such as the above behave during the period of study in that location (Mostly cloudy conditions or not? Air masses passing over ice? etc). Ideally there should be some analysis of the photolysis rates themselves -

in addition to the concentrations and chemical fluxes - but if that is not possible, at least some discussion would be useful to the reader.

We did not present a discussion and evaluation of photolysis in the models, since this is presented in the POLMIP overview paper (Emmons et al., 2014). This paper was submitted and appeared in ACPD some time after submission of our manuscript, so its content may have been unavailable to the reviewer. Briefly, Emmons et al., (2014) describe the treatment of photolysis in the models, show differences between model cloud fractions and $J(O^1D)$ and $J(NO_2)$ photolysis rates, and compare these with ARCTAS data from the NASA DC8 aircraft. We do not feel that it is worthwhile repeating this analysis here. However, we have added text in the penultimate paragraph of Section 3.2 to explicitly highlight that differences in simulated photolysis rates likely contribute to differences in ozone production efficiency relative to high latitude CO enhancement:

"**Differences in simulated photolysis between the models are likely contributors to model spread in photochemical ozone enhancement relative to CO. Such differences are presented and explored for the POLMIP models by Emmons et al., (2014).**"

- Ozone-CO correlations/slopes can be very useful, but being positive is not always indicative of net ozone producing regions, especially over remote areas (as suggested by Voulgarakis et al. (2011) and later also discussed by Kim et al. (2013) and Zhang et al. (2014)). Examining the OH levels in comparison to the background and subsequent CO destruction fluxes would give an indication on the validity of this approach.

This same point was also raised Reviewer 1. We have addressed the point by evaluating the simulated photochemical loss rate of CO in the air masses and compared it with the photochemical ozone production tendency. See our response to Reviewer 1 above.

MINOR COMMENTS:
Page 24580, Lines 6-7: A little more justification of the choice of a 25-day lifetime is needed, for the more general readership.

The 25-day lifetime is somewhat arbitrary, but has been chosen in order to produce tracers with an atmospheric lifetime that is sufficiently long compared with characteristic transport timescales for long-range transport from source regions to the Arctic (a few days to a week), but short enough to avoid a homogeneous well-mixed abundance accumulating during the simulation. A lifetime of 25 days is shorter than the expected range in lifetime of CO corresponding to a range in tropospheric [OH] of between 1.0×10^6 and 2.0×10^6 molec cm^{-3} (roughly 35-80 days). We have added the following sentence to the manuscript: **"A 25-day tracer lifetime is sufficiently long relative to the transport timescale for long-range transport from mid-latitudes to the Arctic (days to a week), while being short enough to avoid the formation of a homogeneous well-mixed tracer distribution."**

Figures 1-4: It would be good to clearly label the axes, i.e. which one is the observations and which one is the model?

Extra labels have been added to more clearly designate model and observations in these figures.

Page 24582, Lines 4-6: Worth mentioning that models typically underestimate CO in the northern extratropics, e.g. see Naik et al. (2013), Fig. 2 for a recent multi-model comparison.

We have added a short section to the text: "**Global models typically underestimate CO in the northern extratropics. A recent multi-model study showed negative annual mean model biases exceeding -45 ppbv compared with surface CO observations at high latitudes, and as large as -30 ppbv compared with satellite-retrieved CO concentrations at 500 hPa over the extra-tropical oceans (Naik et al, 2013).**"

Page 24583, Line 4: Please spell out "oVOC" as it is the first time it is encountered in the text.

Done. Also removed redundant spelling out of oVOC later in manuscript (page 24594, line 12).

Page 24583, Lines 4-7: Any ideas on why oVOCs show such a large variability? Is it a result of different emissions, or of atmospheric processing?

Emissions of these species (acetaldehyde, acetone) are the same for all models – with the exception of some differences for GEOS-Chem and TM5 (see Table 2 in Emmons et al., 2014). The large diversity between the majority of models is therefore a result of differences in photochemical production of these species, due to both differences in treatments of organic chemistry and differences in rates of photochemical processing of parent VOCs that go on to produce these species, as well as differences in their photolysis and OH loss. We have added the following text to the paper to point this out explicitly: **"With the exception of the GEOS-Chem and TM5 models, emissions of acetone and acetaldehyde are the same for all models. The large diversity in model concentrations of these species therefore mainly results from different treatments of organic chemistry, differences in rates of photochemical processing of their parent VOCs and differences in their photolysis and OH loss."**

Figure 4: For SMHI-MATCH the bias appears positive (95%), but visually the figure suggests a negative bias.

The percentage figures quoted in the panels of Figures 1-4 were mean bias. These values were therefore heavily weighted by any points with particularly large bias, even if there are few of them. This was the case for the SMHI-MATCH model in this figure where the maximum bias is 55,000%, leading to a positive mean bias despite most points having a negative bias. We have modified the plots to show median bias instead, to remove this effect.

Figure 5: "(k)" should not be bold.

Corrected.

Figure 6: I would suggest using consistent colouring for young/aged in Figures 5 & 6.

Agree with this suggestion. We have adjusted the colours used in Figure 6 to be consistent with Figure 5.

Figures 5 & 7: In those figures, some model names are different to previous figures.

We have amended model names used, and checked that these are consistent throughout the manuscript.

Page 24587, Lines 22-24: I presume the authors here imply how future model developments regarding convection could affect the results. This should be more clearly stated.

No – this statement refers to the implementation of convective vertical transport in the models as used in the study. The point being made is that during a period of increased convective activity, vertical redistribution of tracer due to convection may partially mask any differences in tracer vertical profile produced by differences in large-scale resolved vertical motion in the driving meteorological data. In many global models, such convective transport is parameterised. We have modified the statement to make its meaning clearer: **"Increased convective vertical mixing in the models may therefore mask some of the differences in vertical tracer structure produced by differences in large-scale vertical transport."**

Page 24589, Line 13: Please change "represented" to "be represented".
Done.

Page 24590, Lines 10-13: It is not clear to me that this is the case. E.g. the CIFS model looks much more similar to TM5 next to it or CAM5 above it rather than to SMHI-MATCH.
This statement refers specifically to the sharpness of gradients in the CO tracer structure close to source regions, and not to tracer concentration values. While the concentration values for CIFS appear more similar to TM5 and CAM5, at least visually there is evidence that there are sharper gradients in filamentary structures close to the E Asia coast (e.g. over the Sea of Okhotsk, to the north of Japan) in the CIFS model on a comparable scale with those in SMHI-MATCH. However, in our analysis we have not made a quantitative assessment of the comparability of these structures and gradients. We feel therefore that this statement was perhaps overly subjective, and so have removed the sentence in question from the manuscript. This does not at all change the key aspects of our discussion or conclusions of our results.

Table 2: It would be useful to show OH on this table too, in order to get a sense of the variability between the models.

OH has been added to the table as suggested.

Page 24594, Lines 13-18: Is the factor of 2 arbitrary or based on the typical diversity range in the POLMIP models (e.g. from Emmons et al., 2014)? Please clarify.

The choice of a factor 2 is somewhat arbitrary, but is consistent with the magnitude of inter-model diversity shown for several species (PAN, oVOCs) along the DC8 flight tracks in Emmons et al., (2014). We chose to apply the same fractional perturbation to each species to allow direct comparison of the relative sensitivity of ozone production their abundances. We have modified the text to clarify this point: **"A factor 2 perturbation is consistent with inter-model differences and biases along the ARCTAS DC8 flight tracks (Emmons et al., 2014). We apply the same fractional perturbation to each species to directly compare sensitivities of Arctic ozone photochemistry to uncertainties in their abundances."**

Page 24595, Lines 3-6: I am not sure I understand, though I may be missing something here: All the lines in Figure 14c seem to be below the zero line, so I am not sure where one can see an enhancement of ozone.

We apologise, as the intended meaning of this text is somewhat unclear and/or misleading. The point is that e.g. the negative perturbation to oVOCs produces an

enhancement to ozone relative to the control case with unperturbed oVOCs, which is demonstrated by a smaller net loss in ozone over the 4-day period – this is not necessarily an enhancement in ozone relative to initial ozone concentration. We have reworded this sentence to improve clarity of intended meaning: **"Increasing and decreasing initial oVOC abundances leads to enhancement and suppression of ozone loss in the plume respectively over the following 4 days (Fig. 14c and d), due to the role of acetaldehyde and acetone as a source of the peroxyacetyl radical during their photo-oxidation."**

Page 24595, Line 16: Please change "changes the rate" to "changes of the rate".

Done (changed "to the rate").

Page 24596, Line 11: Please change "differences efficiency" to "differences in the efficiency".

Done.

References

Mao, J., Fan, S., Jacob, D. J., and Travis, K. R.: Radical loss in the atmosphere from Cu-Fe redox coupling in aerosols, Atmos. Chem. Phys., 13, 509–519, doi:10.5194/acp-13-509-2013, 2013.

Naik, V., Voulgarakis, A., Fiore, A. M., Horowitz, L. W., Lamarque, J.-F., Lin, M., Prather, M. J., Young, P. J., Bergmann, D., Cameron-Smith, P. J., Cionni, I., Collins, W. J., Dalsøren, S. B., Doherty, R., Eyring, V., Faluvegi, G., Folberth, G. A., Josse, B., Lee, Y. H., MacKenzie, I. A., Nagashima, T., van Noije, T. P. C., Plummer, D. A., Righi, M., Rumbold, S. T., Skeie, R., Shindell, D. T., Stevenson, D. S., Strode, S., Sudo, K., Szopa, S., and Zeng, G.: Preindustrial to present-day changes in tropospheric hydroxyl radical and methane lifetime from the Atmospheric Chemistry and Climate Model Intercomparison Project (ACCMIP), Atmos. Chem. Phys., 13, 5277-5298, doi:10.5194/acp-13-5277-2013, 2013.

Voulgarakis, A., Telford, P. J., Aghedo, A. M., Braesicke, P., Faluvegi, G., Abraham, N. L., Bowman, K. W., Pyle, J. A., and Shindell, D. T.: Global multi-year O3-CO correlation patterns from models and TES satellite observations, Atmos. Chem. Phys., 11, 5819-5838, doi:10.5194/acp-11-5819-2011, 2011. Kim, P. S., Jacob, D. J., Liu, X., Warner, J. X., Yang, K., Chance, K., Thouret, V., and Nedelec, P.: Global ozone–CO correlations from OMI and AIRS: constraints on tropospheric ozone sources, Atmos. Chem. Phys., 13, 9321-9335, doi:10.5194/acp-13-9321-2013, 2013.

Zhang, B., Owen, R. C., Perlinger, J. A., Kumar, A., Wu, S., Val Martin, M., Kramer, L., Helmig, D., and Honrath, R. E.: A semi-Lagrangian view of ozone production tendency in North American outflow in the summers of 2009 and 2010, Atmos. Chem. Phys., 14, 2267-2287, doi:10.5194/acp-14-2267-2014, 2014.

List of Manuscript Changes
(line numbers correspond to marked-up manuscript version below)

Line 39 “to” added to slope ranges.

Line 39 corrected slope ranges to be consistent with manuscript.

Line 40 “in” added (response to reviewer).

Lines 159-166 new text added in response to reviewer comment.

Lines 169-172 new text added in response to reviewer comment.

Lines 211-213 text modified to discuss median model bias rather than mean model bias, to be consistent with new versions of Figs. 1-4.

Lines 215-219 new text added in response to reviewer comment.

Lines 234-236 text modified to discuss median model bias rather than mean model bias, to be consistent with new versions of Figs. 1-4.

Lines 241-244 text modified to discuss median model bias rather than mean model bias, to be consistent with new versions of Figs. 1-4.

Lines 249-250 text modified to discuss median model bias rather than mean model bias, to be consistent with new versions of Figs. 1-4.

Line 252 added “oxygenated (o)VOC” in response to reviewer comment.

Lines 255-258 new text added in response to reviewer comment.

Lines 273-274 text modified to discuss median model bias rather than mean model bias, to be consistent with new versions of Figs. 1-4.

Lines 293-301 new text added in response to reviewer comment.

Lines 318-319 text changed “median” to “mean”, since the mean ln(propane/ethane) ratio was actually used to define age classes, not median as was erroneously stated in the earlier version.

Lines 357-359 new text added in response to reviewer comment.

Lines 402-405 text on convective vertical mixing modified in response to reviewer comment.

Lines 430-431 text on GEOS-Chem NOy partitioning removed in response to reviewer comment.

Line 447 “be” added in response to reviewer comment.

Line 475 text removed in response to reviewer comment.

Lines 504-506 text modified to correct description of plume maxima definition, which was incorrectly described in earlier version.

Line 591 “oxygenated” removed as now defined earlier.

Lines 593-597 text modified to clarify motivation for factor 2 perturbation (in response to reviewer comment).

Lines 618-621 text modified to clarify ozone change produced by oVOC perturbations, in response to reviewer comment.

Line 630 “to” added in response to reviewer comment.

Line 657 “in the” added in response to reviewer comment.

Throughout: model names tweaked to be consistent throughout manuscript.

Line 687, 695-697 text added to Acknowledgements.

Lines 771-772 additional reference added.

Lines 786-793 additional reference added.

Lines 877-879 additional reference added.

Lines 899-902 additional reference added.

Table 1: Model names modified to be consistent with manuscript text.

Table 2: Model names modified to be consistent with manuscript text.

Table 2: Plume locations in CAM-Chem model corrected. Error in previous version of Table.

Table 2: OH concentrations added in response to reviewer comment.

Figures 1-4: Bias figures changed from mean to median, in response to reviewer comment.
Axes updated to more clearly label observations and models.

Figure 5: colours modified to be consistent with Figure 6 in response to reviewer comment.

Figure 5: significant figures truncated in response to reviewer comment.

Figure 5 caption text updated to reflect modified colours and use of mean ln(propane/ethane) ratio for age class definition.

Figure 7: significant figures truncated in response to reviewer comment.

Figures 1-4, 7-14: model names corrected to be consistent with text.

Biomass burning influence on high latitude tropospheric ozone and reactive nitrogen in summer 2008: a multi-model analysis based on POLMIP simulations.

S.R. Arnold[1*], L.K. Emmons[2], S.A. Monks[1], K.S. Law[3], D.A. Ridley[4], S. Turquety[5], S. Tilmes[2], J.L. Thomas[3], I. Bouarar[3], J. Flemming[6], V. Huijnen[7], J. Mao[8], B.N. Duncan[9], S. Steenrod[9], Y. Yoshida[9], J. Langner[10], Y. Long[5]

1. Institute for Climate and Atmospheric Science, School of Earth & Environment, University of Leeds, UK.
2. Atmospheric Chemistry Division, NCAR, USA.
3. UPMC Univ. Paris 06; Université Versailles St-Quentin; CNRS/INSU; UMR 8190, Paris, France.
4. Department of Civil and Environmental Engineering, Massachusetts Institute of Technology, Cambridge, MA, USA.
5. Laboratoire de Météorologie Dynamique, IPSL, CNRS, UMR8539, 91128 Palaiseau Cedex, France.
6. ECMWF, Reading, UK.
7. Royal Netherlands Meteorological Institute (KNMI), De Bilt, The Netherlands.
8. Program in Atmospheric and Oceanic Sciences, Princeton University and Geophysical Fluid Dynamics Laboratory/National Oceanic and Atmospheric Administration, Princeton, New Jersey, USA.
9. NASA Goddard Space Flight Center, Greenbelt, MD, USA.
10. Swedish Meteorological and Hydrological Institute, 60176 Norrkö ping, Sweden.

*Correspondence to: s.arnold@leeds.ac.uk

Steve 28/4/2015 08:39
Formatted: Font:10 pt

Steve 28/4/2015 08:40
Deleted:

Steve 28/4/2015 08:39
Deleted:

Abstract

We have evaluated tropospheric ozone enhancement in air dominated by biomass burning emissions at high laititudes (> 50N) in July 2008, using 10 global chemical transport model simulations from the POLMIP multi-model comparison exercise. In model air masses dominated by fire emissions, $\Delta O_3/\Delta CO$ values ranged between 0.039 and 0.196 ppbv/ppbv (mean: 0.113 ppbv/ppbv) in freshly fire-influenced air, and between 0.140 and 0.261 ppbv/ppbv (mean: 0.193 ppbv) in more aged fire-influenced air. These values are in broad agreement with the range of observational estimates from the literature. Model ΔPAN/ΔCO enhancement ratios show distinct groupings according to the meteorological data used to drive the models. ECMWF-forced models produce larger ΔPAN/ΔCO values (4.47 to 7.00 pptv/ppbv) than GEOS5-forced models (1.87 to 3.28 pptv/ppbv), which we show is likely linked to differences in efficiency of vertical transport during poleward export from mid-latitude source regions. Simulations of a large plume of biomass burning and anthropogenic emissions exported from towards the Arctic using a Lagrangian chemical transport model show that 4-day net ozone change in the plume is sensitive to differences in plume chemical composition and plume vertical position among the POLMIP models. In particular, Arctic ozone evolution in the plume is highly sensitive to initial concentrations of PAN, as well as oxygenated VOCs (acetone, acetaldehyde), due to their role in producing the peroxyacetyl radical PAN precursor. Vertical displacement is also important due to its effects on the stability of PAN, and subsequent effect on NOx abundance. In plumes where net ozone production is limited, we find that the lifetime of ozone in the plume is sensitive to hydrogen peroxide loading, due to the production of HO_2 from peroxide photolysis, and the key role of $HO_2 + O_3$ in controlling ozone loss. Overall, our results suggest that emissions from biomass burning lead to large-scale photochemical enhancement in high latitude tropospheric ozone during summer.

Steve 29/4/2015 16:13
Deleted: 4

Steve 28/4/2015 08:52
Deleted: -

Steve 29/4/2015 16:13
Deleted: 6.28

Steve 29/4/2015 16:14
Deleted: 2.02

Steve 28/4/2015 08:52
Deleted: -

Steve 29/4/2015 16:14
Deleted: 02

1. Introduction

Vegetation fires play an important role in ecosystem function and regulation (Bonan, 2008) and contribute substantially to atmospheric CO_2, with gross emissions from biomass burning estimated to be between 2 and 4 PgC a^{-1} globally, equivalent to 40% of those from fossil fuel combustion (Ciais et al., 2013). Biomass burning also impacts atmospheric chemistry, releasing large quantities of aerosol and reactive gas-phase chemical compounds, including CO, NOx (=NO+NO_2) and volatile organic compounds (VOCs) (Andreae et al., 1988; van der Werf et al., 2010). These emissions result in perturbations to tropospheric oxidants, aerosol loading and the atmospheric radiative balance (Dentener et al., 2006). Studies have demonstrated that wildfires in the boreal regions of North America and Eurasia affect abundances of atmospheric trace gases and aerosol at high latitudes (Bourgeois and Bey, 2011; Fisher et al., 2010; Hornbrook et al., 2011; Jaffe and Wigder, 2012; Monks et al., 2012; Paris et al., 2009; Real et al., 2007; Warneke et al., 2010; Wofsy et al., 1992). These contributions peak during spring and summer, when large fires occur naturally in the regions of Alaska and Canada and in central and eastern Siberia (Monks et al., 2012; van der Werf et al., 2010). How anthropogenic and natural sources of climatically-relevant atmospheric constituents will contribute to future high latitude climate change is highly uncertain (Shindell et al., 2008). In particular, our understanding of how boreal fires impact large-scale Arctic and high latitude budgets of climate-relevant atmospheric constituents is limited, and is reliant on sparse observations, often in specific events and isolated plumes. Short-lived climate pollutants (SLCPs) such as tropospheric ozone, aerosol and methane may contribute to accelerated rates of warming observed in the Arctic relative to the global mean temperature increase (Quinn et al., 2008). Changes in tropospheric ozone and aerosol may already have contributed 0.2–0.4°C and 0.5–1.4°C respectively to Arctic surface warming since 1890 (Shindell and Faluvegi, 2009). A better understanding of boreal fire influence on high latitude tropospheric ozone and aerosol is essential for improving the reliability of our projections of future Arctic and northern hemisphere climate change, especially considering proposed climate-fire feedbacks which may enhance the intensity and extent of high latitude wildfire under a warming climate (de Groot et al., 2013).

The role of boreal fires as a source of high latitude tropospheric ozone is particularly poorly constrained, and has been the subject of some controversy, with different studies suggesting both minor and major roles for fires as a source of Arctic ozone. A recent review by (Jaffe and Wigder, 2012) showed that most studies have demonstrated net production of tropospheric ozone from wildfire emissions, due to the propensity of fires to emit large quantities of key ozone precursors (NOx, CO, VOCs). The $\Delta O_3/\Delta CO$ enhancement ratio (defined as the excess ozone mixing ratio above background ozone in an air mass normalized by an enhancement in CO mixing ratio above

background CO), is often used as a measure of ozone production efficiency in fire plumes as they are processed downwind from emission. Values of $\Delta O_3/\Delta CO$ in boreal wildfire plumes from Siberia, Alaska and Canada vary between approximately −0.1 ppbv $ppbv^{-1}$ and 0.6 ppbv $ppbv^{-1}$ (Alvarado et al., 2010; Bertschi et al., 2004; Goode et al., 2000; Honrath et al., 2004; Martin et al., 2006; Mauzerall et al., 1996; Paris et al., 2009; Parrington et al., 2013; Pfister et al., 2006; Real et al., 2007; Singh et al., 2010; Tanimoto et al., 2008; Wofsy et al., 1992). In addition, these values are observed to generally increase with increasing plume age.

A robust estimate of the role of boreal fires in producing tropospheric ozone is hampered by a large range in observational estimates of ozone production efficiency, likely resulting from factors such as variability in emission factors with combustion efficiency and vegetation type, differences in plume age, different plume chemical processing, due to e.g. different aerosol loadings, and mixing with anthropogenic emissions (Jaffe and Wigder, 2012). Integrated analysis of data from multiple boreal fire plumes sampled across Alaska and Canada during the ARCTAS-B campaign concluded that boreal fire emissions had only negligible impact on tropospheric ozone profiles in summer 2008 over Alaska and Canada (Alvarado et al., 2010; Singh et al., 2010). However, plumes sampled were mostly freshly emitted (< 2 days), and box modelling based on the same data suggests high in-situ photochemical production rates, despite little to no measured ozone enhancement in these plumes (Olson et al., 2012). Other recent modelling studies have suggested greater ozone sensitivity to boreal fire emissions in more aged air masses. Tropospheric ozone in coastal Canada has been shown to be highly sensitive to NOx emissions from central Canadian fires (Parrington et al., 2012), and regional modelling for the Arctic in summer 2008 suggests that ozone production increases markedly in fire plumes downwind from emission as air masses process chemically over time (Thomas et al., 2013). Wespes et al., (2012), using a tagged NOx and ozone production scheme in the MOZART-4 global CTM, showed that more than 20% of ozone in the Arctic lower troposphere is produced from NOx emitted from high latitude fires in North America and Asia. Boreal forest fires have also been shown to be an important source of peroxyacetyl nitrate (PAN) in the Arctic during the spring and summer months (Jacob et al., 1992; Singh et al., 2010; Singh et al., 1992). Transport of PAN from lower latitudes into the Arctic makes a substantial contribution to local in-situ ozone production, via NO_2 released from PAN decomposition (Walker et al., 2012).

In light of uncertainties associated with these contributions, there is a need to better evaluate how models simulate the influence of boreal fires on high latitude budgets of ozone and precursors, particularly in summer, when local radiative processes play a major role in Arctic surface temperatures (Shindell, 2007). While several model studies have investigated simulated ozone production from boreal fires, there has been little attempt to understand how differences in model

treatments of chemistry and transport affect estimates of ozone production in fire-influenced air masses.

In this paper, we use results from POLMIP (POLARCAT model intercomparison Project) (Emmons et al., 2014) and observations collected in the Arctic troposphere as part of the ARCTAS-B mission (Jacob et al., 2010), to evaluate simulated summertime tropospheric ozone and its precursors in the northern high latitudes and how it is influenced by boreal fire emissions in a series of state-of-the-art global atmospheric chemical transport models. The POLMIP model experiments and observations used to evaluate them are described in Section 2. In Section 3, we use idealised model tracers to track fire emissions, and compare ozone enhancement ratios ($\Delta O_3/\Delta CO$) in air dominated by fire emission influence across the range of models, and investigate relationships with model NOy partitioning. Section 4 describes a case study of a large biomass burning plume exported from Siberia in July 2008, which we use to investigate the sensitivities of Arctic tropospheric ozone to model chemistry based on Lagrangian chemical model simulations of the plume. Our findings and conclusions are summarised in Section 5.

2. Model simulations and observations

The POLARCAT Model Intercomparison Project (POLMIP) was designed to evaluate the performance of several global and regional–scale chemical transport models (CTMs) in the Arctic troposphere (Emmons et al., 2014). POLMIP contributes to the POLARCAT project aim to better understand model deficiencies identified in a previous evaluation of CTM simulations of Arctic tropospheric ozone and its precursors, and aims to exploit the large amount of observational data collected during the IPY aircraft experiments in the Arctic troposphere during spring and summer 2008. Further details on the POLARCAT project and the 2008 aircraft campaigns are given in Law et al., (2014). All models used the same data for emissions, with the aim of allowing an investigation of model differences due to atmospheric transport and chemical processes only. The exception was the GEOS-Chem model, which used different anthropogenic emissions (Emmons et al., 2014). POLMIP anthropogenic emissions are those provided for the ARCTAS project by D. Streets (Argonne National Lab) and University of Iowa (http://bio.cgrer.uiowa.edu/arctas/emission.html). Daily biomass burning emissions are taken from the Fire Inventory of NCAR (FINN), based on MODIS fire counts (Wiedinmyer et al., 2011). All POLMIP models injected biomass burning emissions into the lowest boundary layer model level, in order to remove any differences produced through treatments of fire emission injection heights. Other emissions (biogenic, ocean, volcano) were derived from the MACCity inventory (Lamarque et al., 2010). Table 1 summarises details of the POLMIP model

simulations used in this study. Further details of the POLMIP model experiments, emissions data and evaluation of the simulations can be found in Emmons et al., (2014).

The GEOS-Chem model includes a parameterization for transition metal-catalysed formation of H_2O from aerosol uptake of HO_2, rather than formation of H_2O_2. This process is effectively an irreversible loss for HOx, and is motivated by the suggestion from field observations that HO_2 uptake to aerosol may not produce H_2O_2. This motivation and the implementation of this scheme are described by Mao et al., (2013b). The same study showed that inclusion of this process reduces the mass-weighted global mean OH concentration by 12%, and substantially increases CO concentrations at high latitudes due to an increased CO lifetime. It was also shown to reduce surface ozone by 3-10 ppbv over North America and Eurasia.

To further aid in understanding inter-model differences in transport, POLMIP models included fixed lifetime tracers from anthropogenic and biomass burning emission sources. A total of 6 tracers were simulated, each with a prescribed fixed atmospheric lifetime of 25 days. A 25-day tracer lifetime is sufficiently long relative to the transport timescale for long-range transport from mid-latitudes to the Arctic (days to a week), while being short enough to avoid the formation of a homogeneous well-mixed tracer distribution. Two tracers were emitted from each of three mid-latitude continental source regions (Europe, North America and Asia), one with the same source as the anthropogenic CO emissions and one from the CO emissions from biomass burning sources. Details on the exact definition of source regions and emission magnitudes are given in Emmons et al., (2014). The Asian biomass burning tracer is dominated by emissions from large Siberian fires in July 2008 (see Emmons et al., 2014). Monks et al. (2012) demonstrated that variability in emissions from boreal fires dominates the inter-annual variability of the ozone precursor, CO in the Arctic troposphere. Using fixed-lifetime CO tracers from the POLMIP simulations, Monks et al., (2014) used these tracers in conjunction with observed and simulated CO to investigate the contributions from differences in model transport and oxidants to inter-model variability in simulated seasonal CO in the Arctic. They showed that emissions from Asian fires are the dominant source of CO tracer in the lower and middle Arctic troposphere, and are approximately equal to the contribution from Asian anthropogenic sources in the upper troposphere. Here, we exploit these tracers to identify regions and periods in the POLMIP model simulations for which air is strongly influenced by fire emissions.

Several aircraft flew missions into the Arctic troposphere during summer 2008 as part of the POLARCAT experiment (Law et al., 2014). The POLARCAT-France and GRACE experiments, based in south-west Greenland sampled aged fire plumes and anthropogenic air masses transported into the Arctic from Siberia and North America. ARCTAS-B, based in central Canada, sampled fresh and aged

Steve 27/4/2015 11:32
Formatted: Subscript

Steve 27/4/2015 11:32
Formatted: Subscript

Steve 27/4/2015 11:32
Formatted: Subscript

Steve 27/4/2015 11:32
Formatted: Subscript

Steve 28/4/2015 08:49
Formatted: Subscript

Steve 27/4/2015 11:32
Formatted: Subscript

Steve 27/4/2015 11:32
Formatted: Subscript

Steve 28/4/2015 08:50
Formatted: Space Before: 0 pt, After: 10 pt

fire emissions over Canada and the Arctic. In this analysis, we make use only of data from the ARCTAS-B mission, for which the NASA DC8 aircraft was equipped with an extensive suite of gas phase and aerosol instrumentation, including ozone, CO, speciated oxides of nitrogen (NOy), volatile organic compounds and peroxides (Jacob et al., 2010). Monks et al., (2014) present a detailed comparison of the POLMIP model simulations with CO and ozone data from all POLARCAT experiments.

During ARCTAS-B, the DC8 aircraft made 7 flights, based from Cold Lake, Canada from 29th June to 10th July 2008. The vast majority of observations were made in fresh Saskatchewan fire plumes, although some flights also targetted aged plumes transported to Canada from Siberian and Californian fires. All ARCTAS DC8 data are available in a publicly accessible archive (http://www-air.larc.nasa.gov/cgi-bin/arcstat-c), and described in Jacob et al., (2010).

3. Fire emission influence on ozone and NOy enhancement in POLMIP models

3.1 Evaluation of model ozone and ozone precursors in air dominated by fire emissions

Using the fixed-lifetime tracers from the models, we evaluate simulations of ozone and precursors against ARCTAS-B aircraft observations in air dominated by fire emissions in the summertime Arctic troposphere. Figures 1-4 respectively show aircraft observations of ozone, CO, PAN and HNO_3 plotted against hourly model output interpolated in time and space to the aircraft position. For each model, points have been coloured according to whether the simulated tracers from fire sources or from anthropogenic sources contribute more than 50% of the total (fire + anthropogenic) tracer mixing ratio at the aircraft location. In model air dominated by fire emissions, simulated ozone generally falls close to the observation-model 1:1 line, and model median biases vary between -22% and +5%, compared with -19% to -2% in anthropogenic-dominated air. As discussed in detail by Monks et al., (2014), all POLMIP models display a negative CO bias, throughout the depth of the troposphere. Use of the POLMIP fixed-lifetime tracers shows that this is the case in both anthropogenic and fire-dominated air. Global models typically underestimate CO in the northern extratropics. A recent multi-model study showed negative annual mean model biases exceeding -45 ppbv compared with surface CO observations at high latitudes, and as large as -30 ppbv compared with satellite- retrieved CO concentrations at 500 hPa over the extra-tropical oceans (Naik et al, 2013). The majority of ARCTAS-B observations were made is fresh biomass burning plumes, leading to larger CO concentrations on average in fire-dominated air masses. The models also simulate larger CO concentrations in these air masses, but with a general underestimate. Monks et al., (2014)

Steve 28/4/2015 17:38
Deleted: 0

Steve 28/4/2015 17:38
Deleted: 7

Steve 28/4/2015 17:40
Deleted: 3

Steve 28/4/2015 17:40
Deleted: +6

Steve 28/4/2015 17:41
Deleted: mean

demonstrated that POLMIP model-simulated global mean OH was generally biased slightly high compared with observational constraints, possibly contributing to their low CO bias.

Simulated distributions of NOy species show some of the largest diversity between models and largest fractional biases against observations. Emmons et al., (2014) showed that POLMIP models display large variability in their budgets of NOy throughout the depth of the Arctic troposphere. The POLMIP models fall into two distinct groups in terms of their simulation of ARCTAS-B PAN concentrations. Models forced by GEOS5 meteorology tend to have lower PAN than observed in fire-dominated air (median biases: -47% to -28%), while the ECMWF-forced models produce PAN concentrations close to or larger than those observed in fire-dominated air (median biases: -2% to +24%). This major difference appears to be related to differences in the efficiency of vertical transport between models using the two different sets of meteorological data (see Section 3.3). Models that transport PAN and its precursors more rapidly to higher altitudes and lower temperatures will likely promote enhanced PAN formation and stability (Singh and Hanst, 1981). These effects on differences in NOy partitioning are explored further in Section 3.3.

GEOS-Chem underestimates DC8 PAN concentrations by the largest magnitude overall (median bias -51%), with lower-than-observed PAN at all locations where observed PAN exceeds 250 pptv. Recent work has substantially improved the simulation of PAN in the GEOS-Chem model (Fischer et al., 2014), however these model updates are not included here. The CIFS model shows very large PAN overestimates (> factor of 4) in fire air masses sampled close to the surface. Comparisons with aircraft observations (see Emmons et al., 2014) show coincident overestimates in NO_2 and acetaldehyde, suggesting these very large PAN concentrations may be partly produced by overestimates in PAN precursors near to fire source regions. In general, the models display substantially larger range in PAN biases in fire-dominated air (median biases: -47% to +24%) compared with anthropogenic-dominated air (median biases: -34% to +5%). Fresh biomass burning plumes observed in ARCTAS-B displayed enhancements in peroxyacetyl precursors such as acetaldehyde and acetone (Hornbrook et al., 2011). Simulated oxygenated (o)VOC enhancements relative to CO (particularly for acetone) in the POLMIP models show large variability close to Canadian fires (Emmons et al., 2014), which may in turn lead to a large range in simulated PAN production. With the exception of the GEOS-Chem and TM5 models, emissions of acetone and acetaldehyde are the same for all models. The large diversity in model concentrations of these species therefore mainly results from different treatments of organic chemistry, differences in rates of photochemical processing of their parent VOCs and differences in their photolysis and OH loss.

Steve 28/4/2015 17:43
Deleted: 37

Steve 28/4/2015 17:43
Deleted: 11

Steve 28/4/2015 17:44
Deleted: more

Steve 28/4/2015 17:45
Deleted: than observed

Steve 28/4/2015 17:44
Deleted: +11

Steve 28/4/2015 17:44
Deleted: 40

Steve 28/4/2015 17:46
Deleted: 43

Steve 28/4/2015 08:32
Deleted: c

Steve 28/4/2015 17:47
Deleted: a large positive PAN bias (mean bias +40%) in fire-dominated air, with

Steve 28/4/2015 17:48
Deleted: 37

Steve 28/4/2015 17:48
Deleted: 40

Steve 28/4/2015 17:49
Deleted: 20

Steve 28/4/2015 17:49
Deleted: 22

Several models show a large positive bias in Arctic HNO_3 concentrations (up to a factor 32 in anthropgenically-dominated air). In an earlier study, Alvarado et al. (2010) used the GEOS-Chem model to study HNO_3 in fire-influenced air masses. This study concluded that the over-prediction of HNO_3 was due to under-prediction of NOx conversion to PAN in fire Influenced air masses. The POLMIP models do no generally support this offsetting of positive biases in HNO_3 with under-prediction of PAN.

Steve 28/4/2015 17:51
Deleted: All

Steve 28/4/2015 17:52
Deleted: The exception is the MOZART-4 model, which has a small negative bias (-9%) in fire-dominated air.

3.2 Model ozone production in fire-dominated Arctic air masses

Previous studies have directly determined the contribution from fire emissions to model ozone by removing emissions from fires (Pfister et al., 2006; Thomas et al., 2013) or by chemically tagging ozone produced by NOx emitted from fires (Wespes et al., 2012). To investigate this contribution in the POLMIP models, we use the 25-day fixed-lifetime tracers to identify the dominant emission source that influences high latitude air in the models. We calculate enhancement in tropospheric ozone as a ratio to CO enhancement ($\Delta O_3/\Delta CO$) where the fixed-lifetime tracers indicate that the model domain is dominated by fire emissions. Points are considered to be fire-dominated where the fire-sourced fixed-lifetime tracer concentration is at least 66% of the total fixed lifetime tracer concentration, and where the fire-sourced fixed-lifetime tracer mixing ratio is at least 10 ppbv. Using this minimum tracer mixing ratio to define air enhanced in fire emissions, we use the slope of CO vs ozone in these air masses to calculate the $\Delta O_3/\Delta CO$ ratio directly. This avoids the definition of a CO mixing ratio enhancement above background CO, which due to OH differences between the models is highly model dependent (Monks et al., 2014).

Recent studies have highlighted the need for caution regarding the use of O_3/CO slopes to diagnose photochemical ozone production, particularly in remote regions, due to slopes being artificially increased by chemical loss of CO due to reaction with OH (e.g. Voulgarakis et al., 2011; Zhang et al., 2014). Chemical rate output from the MOZART-4 model shows that in the domain of our study (latitude 50N-90N, 850-250 hPa) the daily chemical loss rate of CO is small (average 1.9 ppbv/day), equivalent to 1.5%-4.5%. This loss is partly offset by chemical production of CO from VOC oxidation (average 0.9 ppbv/day), and daily fractional rates of chemical ozone production at the same locations are substantially larger (~5 - 45%). This analysis suggests that chemical CO loss is unlikely to have a significant effect on our calculated ozone/CO slopes.

Steve 27/4/2015 11:26
Formatted: Subscript

Steve 28/4/2015 08:50
Formatted: Left, Space After: 10 pt

Using changes in the ratio of concentrations of two co-emitted VOCs with differing atmospheric lifetimes, it is also possible to estimate how model $\Delta O_3/\Delta CO$ values change, as air dominated by fire emissions is transported away from the source region and ages photochemically. For primary-emitted VOCs that have losses dominated by OH-oxidation, the concentration ratio of a more

reactive to a less reactive VOC is expected to reduce over time since emission (Calvert, 1976). Propane (C_3H_8) and ethane (C_2H_6) have respective atmospheric e-folding lifetimes of approximately 5 and 24 days (for an average OH concentration of $2x10^6$ molec/cm^3 (Atkinson et al., 2006)). In the absence of mixing with background concentrations, a decrease in the $\ln([C_3H_8]/[C_2H_6])$ ratio is directly proportional to the time elapsed since emission.

We use the $\ln([C_3H_8]/[C_2H_6])$ ratios from the POLMIP models to create relationships between broad classifications of air mass age and $\Delta O_3/\Delta CO$. Based on model values of the $\ln([C_3H_8]/[C_2H_6])$ ratio, we separate the distribution of high latitude tropospheric model grid boxes into two populations of 'youngest' (points with $\ln([C_3H_8]/[C_2H_6])$ values larger than the mean) and 'oldest' (points with $\ln([C_3H_8]/[C_2H_6])$ values smaller than the mean) air masses, in terms of their estimated age since emission. Figure 5 shows POLMIP model-simulated relationships between $[O_3]$ and [CO] in fire-dominated air in the high latitude free troposphere (latitude > 50N; 850 hPa > pressure > 250 hPa), with calculated $\Delta O_3/\Delta CO$ slopes in youngest and oldest air mass groups as defined by the $\ln([C_3H_8]/[C_2H_6])$ ratios. The SMHI-MATCH and GEOS-Chem models respectively did not explicitly simulate propane and the fixed-lifetime source tracers. Therefore, it is not possible to calculate $\Delta O_3/\Delta CO$ slopes in fire-dominated air according to these age classes.

POLMIP model $\Delta O_3/\Delta CO$ slopes are positive in both the younger and aged fire-dominated air in all models. Slopes in the aged air masses (mean: 0.193 , min: 0.140, max: 0.261 ppbv/ppbv) are larger on average compared with slopes in the younger air masses (mean: 0.113 , min: 0.039, max: 0.196 ppbv/ppbv). This is indicative of photochemical ozone production in fire emission-dominated air emitted into and advected to high latitudes in the POLMIP models, with an increase in ozone enhancement relative to CO enhancement in these air masses as they age photochemically. Two models (TOMCAT and CAM5-Chem) show a slight decrease in $\Delta O_3/\Delta CO$ with air mass age defined by the $\ln([C_3H_8]/[C_2H_6])$ ratio. Supplementary Fig. S1 shows that the ln([propane]/[ethane]) ratio for these models show less distinct separation in their corresponding fire tracer concentrations between the 'young' and 'old' age classes. This suggests that the $\ln([C_3H_8]/[C_2H_6])$ ratio may be a less robust proxy for photochemical age since emission in these models. Figure 5k shows ozone and CO observations from ARCTAS-B DC8 flights over-plotted with $\Delta O_3/\Delta CO$ slopes from the different POLMIP models. Although the DC8 aircraft sampled only a small proportion of the fire-dominated domain simulated by the models, the aircraft points lie close to the model $\Delta O_3/\Delta CO$ slopes. Observed ozone concentrations appear slightly larger as a function of CO than those in the POLMIP simulations. There is also evidence that observed air masses show a larger range in ozone enhancements for a given range of CO enhancement than those simulated, perhaps reflecting a diverse range of fresh plumes sampled by the aircraft close to the fires on the model sub-grid scale.

Steve 28/4/2015 11:13
Deleted: median)

Steve 28/4/2015 11:13
Deleted: median

Steve 28/4/2015 08:37
Deleted: c

POLMIP model $\Delta O_3/\Delta CO$ values are highly consistent compared with the wide range of $\Delta O_3/\Delta CO$ values determined from observational studies in boreal fire plumes. Figure 6 compares the $\Delta O_3/\Delta CO$ values from the POLMIP models with $\Delta O_3/\Delta CO$ values from previous model and observational studies on fire plumes at high latitudes. Average $\Delta O_3/\Delta CO$ values from a previous GEOS-Chem model study based on ARCTAS-B range between -0.07 and 0.01 (Alvarado et al., 2010), substantially smaller than values from the POLMIP models. Moreover, these values indicate a tendency for ozone loss in fire plumes, however these values were diagnosed in freshly fire-influenced air masses. The POLMIP models agree well with regional WRF-chem model simulations for the ARCTAS-B campaign, which produced mean $\Delta O_3/\Delta CO$ values in fresh and aged biomass burning plumes of 0.08 and 0.49 ppbv/ppbv respectively, and used the same FINN fire emissions as the POLMIP models (Thomas et al., 2013). Differences in simulated photolysis between the POLMIP models are likely contributors to model spread in photochemical ozone enhancement relative to CO. Such differences are presented and explored for the POLMIP models by Emmons et al., (2014). Mao et al., (2013a), using the GFDL AM3 model with aerosol loss uptake of HO_2, characterized a suppressed large-scale ozone enhancement from fires ($\Delta O_3/\Delta CO = 0.16$) at high latitudes (> 60N) compared with the tropics. This is also seen in comparisons of observational studies between different latitudes, however observed $\Delta O_3/\Delta CO$ at high latitudes is often larger than this large-scale average value derived from their model (Jaffe and Wigder, 2012). Both heterogeneous HO_2 loss on aerosol (Mao et al., 2013) and bromine chemistry (Parrella et al., 2012), implemented in GEOS-Chem for POLMIP may also play a role in reducing tropospheric ozone abundance.

Overlaying O_3/CO slopes from the other POLMIP models onto plots of GEOS-Chem and SMHI-MATCH $[O_3]$ vs [CO] allows some comparison of their efficiency of Arctic tropospheric $[O_3]$ production with other POLMIP models. POLMIP model O_3/CO slopes lie through the $[O_3]$ vs [CO] distribution from the SMHI-MATCH model, which at larger [CO], shows a slope value consistent with the smaller slope values from other POLMIP models. GEOS-Chem shows the lowest ozone enhancement as a function of CO among the POLMIP models, outside of the range of the majority of other models and the ARCTAS-B observations.

3.3 High latitude PAN enhancement in POLMIP models

Enhancements in PAN relative to CO in the high latitude troposphere in the POLMIP models show grouping according to the source of meteorological data used to drive the models. Analogous to the ozone enhancement ratio ($\Delta O_3/\Delta CO$), $\Delta PAN/\Delta CO$ can be used to evaluate the efficiency of PAN formation and its transport to high latitudes in the POLMIP models (Fig. 7). Observations show that

PAN was the dominant NOy component in the Arctic troposphere during summer 2008 (Alvarado et al., 2010; Liang et al., 2011), and as a source of NOx, may be an important driver of tropospheric ozone production at high latitudes (Walker et al., 2012). Average ΔPAN/ΔCO values in GEOS5-forced models range between 1.87-3.28 pptv/ppbv, and in ECMWF-forced models range between 4.47-7.00 pptv/ppbv. Along with the biases shown in Fig. 3, this further suggests that major differences in summertime NOy partitioning may be driven by differences in model vertical transport efficiency. While differences in PAN abundances in the Arctic troposphere shown in Fig. 3 could be explained by differences in efficiency of poleward pollution transport in the models generally, differences in ΔPAN/ΔCO slopes reflect inter-model variability in the efficiency of PAN production or transport relative to CO. CO has a long atmospheric lifetime relative to the transport timescales characteristic of poleward frontal export, and is dominated by primary emissions. Therefore, ΔPAN/ΔCO variability likely represents differences in the rate of PAN formation and its stability. This may be driven by different efficiencies of air mass uplift during boundary layer export, promoting PAN stability, or differences in organic chemistry, controlling the abundance of the acetyl peroxy radical precursor.

The vertical distributions of the 25-day fixed-lifetime CO tracers in the models indicate a more vertically well-mixed lower troposphere in the ECMWF models compared with the GEOS-5 models in general. Figure 8 shows zonal mean differences in tracers between 900hPa and 500hPa at northern hemisphere mid-latitudes in spring and summer. In spring, TOMCAT, TM5 and CIFS show a weaker vertical tracer gradient than CAM4-Chem, CAM5-Chem, MOZART-4 and GMI, suggesting less efficient vertical transport in the GEOS5-driven models over mid-latitude source regions. This pattern is less clear in summer, however between 45 and 55^{O}N this general behaviour is evident among the same models, with the exception of MOZART-4, which becomes more vertically well-mixed. Mid-latitude convection is likely more important for vertical transport in summer. Increased convective vertical mixing in the models may therefore mask some of the differences in vertical tracer structure produced by differences in large-scale vertical transport.

Average values of ΔPAN/ΔCO from a range of fresh and aged fire plumes sampled during ARCTAS-B varied between 2.8 and 0.35 pptv/ppbv (Alvarado et al., 2010), in better agreement with values produced by the GEOS5-driven models. Figure 7k shows PAN and CO from ARCTAS-B observations. Observed PAN / CO slopes are broadly consistent with those simulated by the POLMIP models. The majority of observations support larger slopes consistent with the ECMWF-driven models. The largest PAN enhancements are produced by the CIFS model, which also shows the largest overall positive bias (+40%) against high latitude PAN observations (Fig. 3). Three POLMIP models use identical chemistry schemes (MOZART-4, CAM4-Chem, CAM5Chem). Among these three models,

Steve 28/4/2015 08:50
Formatted: Line spacing: 1.5 lines

Steve 28/4/2015 08:34
Deleted:

Steve 27/4/2015 11:59
Deleted: Parameterisation of sub-grid convection in the models therefore may mask some of the differences in large-scale vertical transport characteristic of the driving meteorological data.

ΔPAN/ΔCO values increase from 1.91 to 3.55 pptv/ppbv, and $\Delta O_3/\Delta CO$ enhancements increase with this increasing Arctic PAN import efficiency. Across all POLMIP models, we see no robust relationship between increased Arctic PAN import efficiency and increased ozone production efficiency ($\Delta O_3/\Delta CO$). Differences in photochemistry between the models likely determine the efficiency with which NOy import is manifested in high laittude ozone enhancement. In addition, a reduction in NOx through more rapid PAN formation in the ECMWF models, and consequent suppression of ozone production in plumes transported poleward may also play a role (Jacob et al., 1992; Mauzerall et al., 1996).

The NOy biases shown by GEOS-Chem are consistent with those shown in Alvarado et al. (2010), who found that PAN and HNO_3 in the GEOS-Chem model were under- and over-estimated respectively by almost a factor 2. In particular, the large negative bias in high latitude PAN (Fig. 3) may explain the lower ozone enhancement compared with other POLMIP models. This bias is largest among the POLMIP models. The simulated low PAN abundances are unlikely explained by the composition of emissions, since all POLMIP models use the same fire emissions.

Steve 27/4/2015 11:37

Deleted: , despite GEOS-Chem directly emitting 40% of fire NOx as PAN and 20% of fire NOx as HNO_3 to capture observed rapid conversion of NOx to NOy in fire plumes.

4. Arctic fire plume sensitivities to model chemistry

In order to further investigate the sensitivities of high latitude tropospheric ozone production to differences in POLMIP model NOy partitioning and photochemistry in fire plumes, we analyse chemical processing during the export of a large plume of Siberian biomass burning and anthropogenic emissions from Asia to the Arctic. By carrying out additional simulations using a Lagrangian chemical transport model, we quantify how differences in chemical composition of this plume between the POLMIP models following export from Asia and poleward transport, and differences in subsequent transport in the Arctic, impact the evolution of ozone in the plume.

4.1 Siberian biomass burning & Asian anthropogenic plume case study

Between 6th and 9th July 2008, a low-pressure system travelled from Siberia across the Arctic Ocean towards the North Pole, carrying with it smoke plumes from Siberian wildfires and emissions from anthropogenic sources in East Asia. This extensive plume of polluted air was sampled both remotely from satellite and by aircraft in-situ measurements. The IASI (Infrared Atmospheric Sounding Interferometer) satellite instrument observed the plume as a large feature of enhanced CO that was exported from the Asian east coast and advanced towards the North Pole (Pommier et al., 2010). On 6 and 7 July the plume was between 850 km and 1600 km wide, large enough to be represented on the grid-scale of the POLMIP global models. As part of ARCTAS-B, the DC8 aircraft also sampled the plume on 9th July, between 80 and 85^{O}N, to the north of Greenland. Despite excessive diffusion in the polar region due to the singularity at the pole on the Eulerian global grid, Sodemann et al.,

(2011) showed that the TOMCAT global model was able to capture the large-scale export of the plume, its horizontal position, and its poleward transport into the Arctic region. This event provides a good case study for evaluation of differences in transport and chemistry of fire-influenced pollution to the Arctic among the POLMIP models.

The general horizontal position, size and shape of the plume agree well between the different POLMIP model simulations. This is likely due to the use of the same emissions data in each model, and large-scale horizontal flow associated with the low pressure system being largely consistent between different driving meteorological data. Figure 9 shows total column CO from the POLMIP models at 06:00UT on 7th July 2008, just as the leading edge of the plume reaches 80^{O}N, at ~180 ^{O}W. The plume extent and position simulated by the POLMIP models is also consistent with the observed IASI satellite CO columns (Sodemann et al., 2011). The positions and relative enhancement of simulated column CO maxima are controlled by simulated horizontal transport and diffusive processes at the sub-plume scale, but also vertical transport processes which control the export CO from the boundary layer and the extent to which exported pollution layers remain distinct or become vertically diffusive.

There are large differences in the magnitude of CO simulated in the plume. Differences in model OH have been shown to have a strong influence on inter-model variability in Arctic CO in the POLMIP models (Monks et al., 2014). These same differences are evident in Fig. 9, particularly in CO column differences in Arctic background air surrounding the plume enhancements. Figures 10 and 11 show column distributions of 25-day lifetime tracers emitted from Asian anthropogenic and Asian fire sources respectively. The lower resolution models tend to simulate more diffuse and poleward penetration of anthropogenic-emitted tracer into the Arctic compared with the CIFS model.

Steve 27/4/2015 12:02

Deleted: The enhanced horizontal resolution of the CIFS and SMHI-MATCH models results in the retention of more distinct filamentary tracer structures close to and downstream from source regions, compared with more diffusive structures in the other models.

Although the plume appears as a largely coherent single feature in total column CO, the fixed-lifetime tracers reveal large-scale separation of anthropogenic and fire contributions. The leading edge of the plume in all models is dominated by fire emissions, with the main part of the anthropogenically-sourced air mass further to the south (Fig. 10). Backward modelling simulations with the FLEXPART Lagrangian particle dispersion model have also demonstrated that when this plume was sampled by the DC8 aircraft on 9th July 2008, CO contributions from anthropogenic and fire sources showed large-scale separation, with Asian fossil fuel sourced CO dominating above 6-7km altitude (Sodemann et al., 2011). Enhanced CO from the anthropogenic part of this plume was transported into the lowermost stratosphere, and was sampled by the DLR Falcon aircraft during the

POLARCAT-GRACE campaign on 10th July 2008 (Roiger et al., 2011). The separation between anthropogenic and fire influence within the plume is highly consistent across the POLMIP models, suggesting good agreement in the locations of export and large-scale horizontal transport of emissions from these two sources from the Asian boundary layer to the Arctic. The GMI and MOZART-4 model plume maxima are situated at lower altitudes compared to the other models (Table 2), again consistent with less efficient vertical export in GEOS5-driven models (Fig. 8).

4.2 Lagrangian chemical model simulations

From each of the POLMIP global model simulations, the positions of plume maxima are determined from the plume distributions shown in Fig. 9. Maxima locations are determined by locating the model grid that contains the maximum Asian fire tracer mixing ratio in the horizontal and vertical in the region of the simulated plume. Table 2 shows the longitude, latitude and pressure of plume maxima in the POLMIP models at 06:00UT on 7th July 2008, following export from the Asian continental boundary layer and import into the Arctic. Table 2 also shows POLMIP model concentrations of key species for ozone photochemistry at these maxima locations. From these maxima locations in each POLMIP model, Lagrangian forward air mass trajectories are calculated using the ROTRAJ (Reading Offline Trajectory) Lagrangian transport model (Methven et al., 2003). Kinematic forward-trajectories from the plume maxima locations are calculated by integration of velocity fields taken from operational analyses of the European Centre for Medium-range Weather Forecasts (ECMWF). The fields at the Lagrangian particle positions are obtained from the 1.0125^{O} horizontal resolution analyses by cubic Lagrange interpolation in the vertical followed by bilinear interpolation in the horizontal and linear interpolation in time. Five-day forward-trajectories were calculated with position output every 6 h. These trajectories account for large-scale advection by the resolved model winds, and neglect convective and turbulent transport.

Using initial chemical conditions from Table 2, and following the forward trajectories calculated from the plume maxima locations for each POLMIP model, we carry out Lagrangian chemical box model simulations using the CiTTyCAT (Cambridge Tropospheric Trajectory model of Chemistry and Transport) Lagrangian CTM (Pugh et al., 2012). The aim of these simulations is to test the sensitivity of ozone in the plume to differences in the chemical composition and the vertical position of the plume following import into the Arctic. Using the same Lagrangian model, Real et al. (2007) simulated photochemistry in an Alaskan biomass burning plume advected over the North Atlantic Ocean and sampled sequentially by several research aircraft. The model was able to reproduce the observed ozone change in the plume observed between aircraft interceptions. We use the CiTTyCAT

Steve 28/4/2015 13:50
Deleted: defined in the horizontal by the

Steve 28/4/2015 13:50
Deleted: box containing

Steve 28/4/2015 13:49
Deleted: column

Steve 28/4/2015 13:49
Deleted: amount

Steve 28/4/2015 13:49
Deleted: . The vertical maximum in the tracer concentration profile over the same model grid box is then used to determine the vertical positions of the plume maxima.

model in single box mode, with a chemical timestep of 5 minutes and physical conditions taken from the ECMWF trajectory data (position, temperature, specific humidity) updated every 30 minutes. Photochemical kinetic data is updated with information where available from the JPL recommendation (Sander et al., 2011), with further data from IUPAC (Atkinson et al., 2004, 2006; Crowley et al., 2010) and the Leeds Master Chemical Mechanism (http://mcm.leeds.ac.uk). In the absence of adequate observations of aerosol size distribution in the plume, we specify fixed aerosol surface area based on observed aerosol size distributions in the boreal fire plume analysed by Real et al. (2007). This surface area (3.0×10^{-6} cm^2/cm^3) is used to calculate rates of heterogeneous chemistry in the CiTTyCAT plume simulations. In order to isolate sensitivities to chemical composition of the plume, we use a single chemistry scheme in the CiTTyCAT Lagrangian simulations (Pugh et al., 2012), and a single set of meteorological data (ECMWF operational analyses data) to calculate transport of the plume forward from 06:00UT on 7th July 2008.

4.3 Simulated plume ozone change and sensitivities to transport and chemistry

We investigate the range of plume ozone production and loss rates produced by the diversity in chemical initial conditions and forward transport from the plume maxima positions in the POLMIP models. Figure 12a shows simulated 4-day ozone change from the CiTTyCAT model in the plume when initialised by different POLMIP model chemical conditions and when following individual forward trajectories from plume maxima locations. The 4-day evolution of pressure along each of these trajectories is shown in Fig. 12d. The 4-day ozone change differs by ~2.5 ppbv across the range of POLMIP model initial concentrations and forward trajectories, with some models showing near-zero net ozone change (TM5, LMDZ-INCA), while others show net ozone loss of more than 2 ppbv (CAM4-Chem, CAM5-Chem). These differences are produced both by differences in the chemical composition of the plume and different transport pathways forwards over the 4 day period. In particular, differences in plume altitude and subsequent vertical displacement over the 4 days affects the formation and stability of PAN, as well as the balance between ozone production and loss via the reactions of $O(^1D)$ with water vapour and of $O_3 + HO_2$.

All plume simulations result in net ozone loss over 4 days, with ozone destruction dominated by the reaction of $O_3 + HO_2$. The TM5-initialised plume shows very little net ozone change, likely due to its relatively high altitude, suppressing both ozone production due to PAN stability and ozone loss due to the dry upper tropospheric conditions of the Arctic. The GMI-initialised plume shows a large ozone production tendency of 2 ppbv day^{-1} on average, which is balanced by large ozone loss rates of slightly larger but similar magnitude. Larger ozone production tendency is driven by the larger

NOx concentrations in this plume compared to those initialized from the other POLMIP models. Similar strong NOx-limitation of ozone production in Arctic biomass burning plumes was first noted during flights made in western Alaska during the ABLE3A mission (Jacob et al., 1992). The cycle of ozone production and loss rates in this simulation also suggests that the pathway followed by this plume from its initial position favours more efficient photochemistry, due to exposure to relatively more hours of peak solar radiation.

The simulated ozone change shows strong sensitivity to the physical position and displacement of the air mass forward trajectories. Figure 13 shows net changes in ozone and PAN from analogous CiTTyCAT simulations in which forward trajectories from each of the 7 model plume locations have been used in conjunction with the 7 sets of chemical initial conditions from the POLMIP models. This produces an ensemble of 49 Lagrangian model simulations, with varying combinations of chemical composition and physical displacement. This diversity produces a much larger range in ozone change over 4 days (approx.. -5 ppbv to +4 ppbv). Several simulations initialised by chemical conditions from the TOMCAT and GMI models result in net ozone production. These models have plume compositions enhanced in NOx and PAN compared with the other POLMIP models (Table 2). In particular, the conversion of enhanced PAN from the TOMCAT initial state to NOx (Fig. 13b) results in enhanced ozone production in forward trajectories that descend (LMDZ-INCA, MOZART-4) or begin at lower altitudes (GMI) (Fig. 12d).

Additional plume simulations using the CiTTyCAT model and the model-specific forward trajectories, reveal strong sensitivity of ozone in the plume to chemical composition simulated by the POLMIP models. We have investigated separately sensitivity to (a) PAN; (b) oVOCs (acetaldehyde, acetone); and (c) peroxides (H_2O_2, CH_3OOH), using simulations where the initial concentrations of each of these three sets of species from each POLMIP model are decreased and increased by a factor of 2. A factor 2 perturbation is consistent with inter-model differences and biases against observations for these species along the ARCTAS DC8 flight tracks (Emmons et al., 2014). We apply the same fractional perturbation to each species to directly compare sensitivities of Arctic ozone photochemistry to uncertainties in their abundances.

Ozone sensitivities to initial PAN concentration in the plume demonstrate the potential importance of model biases in Arctic NOy for Arctic tropospheric ozone. Figure 14 shows changes in simulated ozone and NOx evolution in the plume produced by simulations with perturbations to initial PAN. Increasing and decreasing initial PAN abundance in the plume leads to a reduction in NOx and an increase in NO_X respectively (Fig. 14b). The consequent impacts on ozone change in the plume largely depend on the absolute NOx concentration, and the magnitude of the NOx perturbation

Steve 28/4/2015 08:51
Formatted: Left, Space After: 10 pt

Steve 27/4/2015 11:54
Deleted: oxygenated (

Steve 27/4/2015 11:54
Deleted:)

Steve 27/4/2015 12:04
Deleted: These species were shown to have large inter-model differences and biases against observations in the POLMIP model experiments (Emmons et al., 2014), and the aim here is to investigate the extent to which uncertainties in their modelled abundances may affect simulation of Arctic ozone.

brought about by the fractional change in initial PAN. In the TOMCAT, LMDZ-INCA and GMI-initialised plumes, an increase in initial PAN leads to a shift from slight net ozone loss to net ozone production of between 0.5 and 1 ppbv over 4 days (Fig. 14b). Model plumes that descend over the 4 days have increased NOx sensitivity to the PAN perturbation. Such altitude changes promote reduced PAN stability and release of NO_2. This illustrates the potential sensitivity of in-situ Arctic ozone production in the simulated fire plume to model NOy partitioning errors. Increasing and decreasing initial oVOC abundances leads to enhancement and suppression of ozone loss in the plume respectively over the following 4 days (Fig. 14c and d), due to the role of acetaldehyde and acetone as a source of the peroxyacetyl radical during their photo-oxidation. This promotes the formation of PAN, reducing NOx concentrations in the plume. Consequently, model plumes in which NOx concentrations are large enough to promote ozone production show larger ozone sensitivity to this perturbation. These results suggest that after having undergone export from the continental boundary layer and long-range transport into the Arctic, PAN formation and loss may still play an important role in ozone photochemistry in such plumes. In plumes with very low NOx abundances, and dominated by ozone loss, perturbation to initial peroxide concentrations produces a larger effect on ozone (approx. ±0.5 ppbv over 4 days in the CAM5-chem plume) (Fig. 14e). Increased and decreased peroxide leads to increases and decreases in HO_2 production from peroxide photolysis, resulting in changes to the rate of ozone loss via $O_3 + HO_2$. Increased initial peroxide concentrations also lead to enhanced removal of NOx in the plume, due to increased HOx production (Fig. 14f).

Steve 27/4/2015 12:05
Deleted: Increasing and decreasing initial oVOC abundances leads to suppression and enhancement of ozone in the plume over the following 4 days respectively (Fig. 14c-d), due to the role of acetaldehyde and acetone as a source of the peroxyacetyl radical during their photo-oxidation.

Steve 27/4/2015 12:05
Formatted: Font color: Auto

5. Summary and conclusions

We have evaluated tropospheric ozone enhancement in air dominated by biomass burning emissions at high laititudes (> 50N) in the summer, using simulations from the POLMIP multi-model comparison exercise for July 2008. Using 25-day fixed lifetime CO tracers emitted from fires and anthropogenic sources in the models, we calculated $\Delta O_3/\Delta CO$ enhancement ratios in air dominated by fire emissions. All POLMIP models that simulated fixed-lifetime tracers demonstrate positive ozone enhancement in fire-dominated air, with ozone enhancement increasing with air mass age on average in the models, suggesting net tropospheric ozone production in biomass burning air masses transported to the Arctic. $\Delta O_3/\Delta CO$ values ranged between 0.039 and 0.196 ppbv/ppbv (mean: 0.113 ppbv/ppbv) in the younger air, and between 0.140 and 0.261 ppbv/ppbv (mean: 0.193 ppbv) in the more aged air, with age since emission defined by the ratio of propane to ethane mixing ratios. These values are in broad agreement with the range of observational estimates from the literature,

and larger than those in some previous modelling studies. Model NOy partitioning may play an important role in determining lower model-diagnosed ozone production efficiencies.

Model ΔPAN/ΔCO enhancement ratios at high latitudes show distinct groupings according to the meteorological data used to drive the models. ECMWF-forced models produce larger ΔPAN/ΔCO values (4.44-6.28 pptv/ppbv) than GEOS5-forced models (2.02-3.02 pptv/ppbv), which we show is likely linked to differences in the efficiency of vertical transport during poleward export from mid-latitude source regions. Comparison with limited observations from the ARCTAS-B aircraft campaign suggests that the larger PAN enhancement ratios simulated by the ECMWF-forced models are consistent with the majority of these observations. We find little relationship between the efficiency of Arctic PAN import in fire-dominated air and Arctic ozone enhancement across the diverse range of POLMIP models. However, among three models using the same chemistry scheme there is a general increase in $\Delta O_3/\Delta CO$ with increased PAN import efficiency.

All POLMIP models are capable of resolving a large plume of mixed Asian anthropogenic and Siberian fire pollution, which is imported to the Arctic on July 7th 2008, with close similarities in simulated horizontal structure. These features are in good agreement with CO observations from the IASI satellite instrument and the FLEXPART Lagrangian particle dispersion model, shown in a previous study (Sodemann et al., 2011). Fixed-lifetime tracers simulated by the models show that the leading edge of this plume is dominated by fire emissions in all POLMIP models. Simulations using a Lagrangian chemical transport model show that 4-day net ozone change in the plume is sensitive to differences in plume chemical composition and plume vertical position among the POLMIP models. In particular, Arctic ozone evolution in the plume is highly sensitive to initial concentrations of PAN, as well as oxygenated VOCs (acetone, acetaldehyde), due to their role in producing the peroxyacetyl radical PAN precursor. Vertical displacement is also important due to its effects on the stability of PAN, and subsequent effect on NOx abundance. In plumes where net ozone production is limited, we find that the lifetime of ozone in the plume is sensitive to hydrogen peroxide loading, due to the production of HO_2 from peroxide photolysis, and the key role of $HO_2 + O_3$ in controlling ozone loss.

Overall, our results suggest that emissions from biomass burning lead to large-scale enhancement in high latitude NOy and tropospheric ozone during summer, with increasing production of ozone as air masses age, and that this is consistent across a wide range of chemical transport models using the same emissions data. In addition, model deficiencies and inter-model differences in simulating species that are less commonly observed in the Arctic (PANs, oxygenated VOCs, and peroxides) are important to understand due to their substantial roles in governing in-situ ozone production and loss in plumes imported to the summertime Arctic troposphere.

Acknowledgements

SRA acknowledges support from the NCAR Advanced Study Program via a Faculty Fellowship award, and the NCAR Atmospheric Chemistry Division. SRA and SAM were supported by the EurEX project, funded by the UK Natural Environment Research Council (ref: NE/H020241/1). LKE and S. Tilmes acknowledge the National Center for Atmospheric Research, which is sponsored by the U.S. National Science Foundation. Author LKE acknowledges support from the National Aeronautics and Space Administration under Award No. NNX08AD22G issued through the Science Mission Directorate, Tropospheric Composition Program. Authors K.S.L., J.L.T., S.Turquety and Y.L. acknowledge support from projects Agence National de Recherche (ANR) Climate Impact of Short-lived Climate Forcers and Methane in the Arctic (CLIMSLIP) Blanc SIMI 5-6 021 01 and CLIMSLIP-LEFE (CNRS-INSU). VH acknowledges funding from the European Union's Seventh Framework Programme (FP7) under Grant Agreement no 283576. Contributions from the Swedish Meteorological and Hydrological Institute were funded by the Swedish Environmental Protection Agency under contract NV-09414-12 and through the Swedish Climate and Clean Air research program, SCAC.

Steve 27/4/2015 15:11
Deleted: as

References

Alvarado, M. J., Logan, J. A., Mao, J., Apel, E., Riemer, D., Blake, D., Cohen, R. C., Min, K. E., Perring, A. E., Browne, E. C., Wooldridge, P. J., Diskin, G. S., Sachse, G. W., Fuelberg, H., Sessions, W. R., Harrigan, D. L., Huey, G., Liao, J., Case-Hanks, A., Jimenez, J. L., Cubison, M. J., Vay, S. A., Weinheimer, A. J., Knapp, D. J., Montzka, D. D., Flocke, F. M., Pollack, I. B., Wennberg, P. O., Kurten, A., Crounse, J., St Clair, J. M., Wisthaler, A., Mikoviny, T., Yantosca, R. M., Carouge, C. C., and Le Sager, P.: Nitrogen oxides and PAN in plumes from boreal fires during ARCTAS-B and their impact on ozone: an integrated analysis of aircraft and satellite observations, Atmospheric Chemistry and Physics, 10, 9739-9760, 2010.

Andreae, M. O., Browell, E. V., Garstang, M., Gregory, G. L., Harriss, R. C., Hill, G. F., Jacob, D. J., Pereira, M. C., Sachse, G. W., Setzer, A. W., Dias, P. L. S., Talbot, R. W., Torres, A. L., and Wofsy, S. C.: Biomass-burning emissions and associated haze layers over Amazonia, Journal of Geophysical Research: Atmospheres, 93, 1509-1527, 1988.

Atkinson, R., Baulch, D. L., Cox, R. A., Crowley, J. N., Hampson, R. F., Hynes, R. G., Jenkin, M. E., Rossi, M. J., Troe, J., and Subcommittee, I.: Evaluated kinetic and photochemical data for atmospheric chemistry: Volume II – gas phase reactions of organic species, Atmos. Chem. Phys., 6, 3625-4055, 2006.

Bertschi, I. T., Jaffe, D. A., Jaegle, L., Price, H. U., and Dennison, J. B.: PHOBEA/ITCT 2002 airborne observations of transpacific transport of ozone, CO, volatile organic compounds, and aerosols to the northeast Pacific: Impacts of Asian anthropogenic and Siberian boreal fire emissions, Journal of Geophysical Research-Atmospheres, 109, 2004.

Bourgeois, Q. and Bey, I.: Pollution transport efficiency toward the Arctic: Sensitivity to aerosol scavenging and source regions, Journal of Geophysical Research-Atmospheres, 116, 2011.

Calvert, J. G.: HYDROCARBON INVOLVEMENT IN PHOTOCHEMICAL SMOG FORMATION IN LOS-ANGELES ATMOSPHERE, Environ. Sci. Technol., 10, 256-262, 1976.

de Groot, W. J., Flannigan, M. D., and Cantin, A. S.: Climate change impacts on future boreal fire regimes, For. Ecol. Manage., 294, 35-44, 2013.

Fischer, E. V., Jacob, D. J., Yantosca, R. M., Sulprizio, M. P., Millet, D. B., Mao, J., Paulot, F., Singh, H. B., Roiger, A., Ries, L., Talbot, R. W., Dzepina, K., and Pandey Deolal, S.: Atmospheric peroxyacetyl nitrate (PAN): a global budget and source attribution, Atmos. Chem. Phys., 14, 2679-2698, 2014.

729 Fisher, J. A., Jacob, D. J., Purdy, M. T., Kopacz, M., Le Sager, P., Carouge, C., Holmes, C. D., Yantosca,
730 R. M., Batchelor, R. L., Strong, K., Diskin, G. S., Fuelberg, H. E., Holloway, J. S., Hyer, E. J., McMillan,
731 W. W., Warner, J., Streets, D. G., Zhang, Q., Wang, Y., and Wu, S.: Source attribution and interannual
732 variability of Arctic pollution in spring constrained by aircraft (ARCTAS, ARCPAC) and satellite (AIRS)
733 observations of carbon monoxide, Atmos. Chem. Phys., 10, 977-996, 2010.
734 Goode, J. G., Yokelson, R. J., Ward, D. E., Susott, R. A., Babbitt, R. E., Davies, M. A., and Hao, W. M.:
735 Measurements of excess O-3, CO2, CO, CH4, C2H4, C2H2, HCN, NO, NH3, HCOOH, CH3COOH, HCHO,
736 and CH3OH in 1997 Alaskan biomass burning plumes by airborne fourier transform infrared
737 spectroscopy (AFTIR), Journal of Geophysical Research-Atmospheres, 105, 22147-22166, 2000.
738 Honrath, R. E., Owen, R. C., Val Martin, M., Reid, J. S., Lapina, K., Fialho, P., Dziobak, M. P., Kleissl, J.,
739 and Westphal, D. L.: Regional and hemispheric impacts of anthropogenic and biomass burning
740 emissions on summertime CO and O3 in the North Atlantic lower free troposphere, Journal of
741 Geophysical Research-Atmospheres, 109, 2004.
742 Hornbrook, R. S., Blake, D. R., Diskin, G. S., Fried, A., Fuelberg, H. E., Meinardi, S., Mikoviny, T.,
743 Richter, D., Sachse, G. W., Vay, S. A., Walega, J., Weibring, P., Weinheimer, A. J., Wiedinmyer, C.,
744 Wisthaler, A., Hills, A., Riemer, D. D., and Apel, E. C.: Observations of nonmethane organic
745 compounds during ARCTAS - Part 1: Biomass burning emissions and plume enhancements,
746 Atmospheric Chemistry and Physics, 11, 11103-11130, 2011.
747 Jacob, D. J., Crawford, J. H., Maring, H., Clarke, A. D., Dibb, J. E., Emmons, L. K., Ferrare, R. A.,
748 Hostetler, C. A., Russell, P. B., Singh, H. B., Thompson, A. M., Shaw, G. E., McCauley, E., Pederson, J.
749 R., and Fisher, J. A.: The Arctic Research of the Composition of the Troposphere from Aircraft and
750 Satellites (ARCTAS) mission: design, execution, and first results, Atmospheric Chemistry and Physics,
751 10, 5191-5212, 2010.
752 Jacob, D. J., Wofsy, S. C., Bakwin, P. S., Fan, S. M., Harriss, R. C., Talbot, R. W., Bradshaw, J. D.,
753 Sandholm, S. T., Singh, H. B., Browell, E. V., Gregory, G. L., Sachse, G. W., Shipham, M. C., Blake, D. R.,
754 and Fitzjarrald, D. R.: Summertime photochemistry of the troposphere at high northern latitudes,
755 Journal of Geophysical Research: Atmospheres, 97, 16421-16431, 1992.
756 Jaffe, D. A. and Wigder, N. L.: Ozone production from wildfires: A critical review, Atmospheric
757 Environment, 51, 1-10, 2012.
758 Lamarque, J. F., Bond, T. C., Eyring, V., Granier, C., Heil, A., Klimont, Z., Lee, D., Liousse, C., Mieville,
759 A., Owen, B., Schultz, M. G., Shindell, D., Smith, S. J., Stehfest, E., Van Aardenne, J., Cooper, O. R.,
760 Kainuma, M., Mahowald, N., McConnell, J. R., Naik, V., Riahi, K., and van Vuuren, D. P.: Historical
761 (1850–2000) gridded anthropogenic and biomass burning emissions of reactive gases and aerosols:
762 methodology and application, Atmos. Chem. Phys., 10, 7017-7039, 2010.
763 Liang, Q., Rodriguez, J. M., Douglass, A. R., Crawford, J. H., Olson, J. R., Apel, E., Bian, H., Blake, D. R.,
764 Brune, W., Chin, M., Colarco, P. R., da Silva, A., Diskin, G. S., Duncan, B. N., Huey, L. G., Knapp, D. J.,
765 Montzka, D. D., Nielsen, J. E., Pawson, S., Riemer, D. D., Weinheimer, A. J., and Wisthaler, A.:
766 Reactive nitrogen, ozone and ozone production in the Arctic troposphere and the impact of
767 stratosphere-troposphere exchange, Atmospheric Chemistry and Physics, 11, 13181-13199, 2011.
768 Mao, J. Q., Horowitz, L. W., Naik, V., Fan, S. M., Liu, J. F., and Fiore, A. M.: Sensitivity of tropospheric
769 oxidants to biomass burning emissions: implications for radiative forcing, Geophysical Research
770 Letters, 40, 1241-1246, 2013a.
771 Mao, J., Fan, S., Jacob, D. J., and Travis, K. R.: Radical loss in the atmosphere from Cu- Fe redox
772 coupling in aerosols, Atmos. Chem. Phys., 13, 509–519, doi:10.5194/acp-13- 509-2013, 2013b.
773 Martin, M. V., Honrath, R. E., Owen, R. C., Pfister, G., Fialho, P., and Barata, F.: Significant
774 enhancements of nitrogen oxides, black carbon, and ozone in the North Atlantic lower free
775 troposphere resulting from North American boreal wildfires, Journal of Geophysical Research-
776 Atmospheres, 111, 2006.
777 Mauzerall, D. L., Jacob, D. J., Fan, S. M., Bradshaw, J. D., Gregory, G. L., Sachse, G. W., and Blake, D.
778 R.: Origin of tropospheric ozone at remote high northern latitudes in summer, Journal of Geophysical
779 Research-Atmospheres, 101, 4175-4188, 1996.

Methven, J., Arnold, S. R., O'Connor, F. M., Barjat, H., Dewey, K., Kent, J., and Brough, N.: Estimating photochemically produced ozone throughout a domain using flight data and a Lagrangian model, Journal of Geophysical Research-Atmospheres, 108, 2003.
Monks, S. A., Arnold, S. R., and Chipperfield, M. P.: Evidence for El Nino-Southern Oscillation (ENSO) influence on Arctic CO interannual variability through biomass burning emissions, Geophysical Research Letters, 39, 2012.
Naik, V., Voulgarakis, A., Fiore, A. M., Horowitz, L. W., Lamarque, J.-F., Lin, M., Prather, M. J., Young, P. J., Bergmann, D., Cameron-Smith, P. J., Cionni, I., Collins, W. J., Dalsøren, S. B., Doherty, R., Eyring, V., Faluvegi, G., Folberth, G. A., Josse, B., Lee, Y. H., MacKenzie, I. A., Nagashima, T., van Noije, T. P. C., Plummer, D. A., Righi, M., Rumbold, S. T., Skeie, R., Shindell, D. T., Stevenson, D. S., Strode, S., Sudo, K., Szopa, S., and Zeng, G.: Preindustrial to present-day changes in tropospheric hydroxyl radical and methane lifetime from the Atmospheric Chemistry and Climate Model Intercomparison Project (ACCMIP), Atmos. Chem. Phys., 13, 5277-5298, doi:10.5194/acp-13-5277-2013, 2013.
Olson, J. R., Crawford, J. H., Brune, W., Mao, J., Ren, X., Fried, A., Anderson, B., Apel, E., Beaver, M., Blake, D., Chen, G., Crounse, J., Dibb, J., Diskin, G., Hall, S. R., Huey, L. G., Knapp, D., Richter, D., Riemer, D., Clair, J. S., Ullmann, K., Walega, J., Weibring, P., Weinheimer, A., Wennberg, P., and Wisthaler, A.: An analysis of fast photochemistry over high northern latitudes during spring and summer using in-situ observations from ARCTAS and TOPSE, Atmospheric Chemistry and Physics, 12, 6799-6825, 2012.
Paris, J. D., Stohl, A., Nedelec, P., Arshinov, M. Y., Panchenko, M. V., Shmargunov, V. P., Law, K. S., Belan, B. D., and Ciais, P.: Wildfire smoke in the Siberian Arctic in summer: source characterization and plume evolution from airborne measurements, Atmospheric Chemistry and Physics, 9, 9315-9327, 2009.
Parrella, J. P., Jacob, D. J., Liang, Q., Zhang, Y., Mickley, L. J., Miller, B., Evans, M. J., Yang, X., Pyle, J. A., Theys, N., and Van Roozendael, M.: Tropospheric bromine chemistry: implications for present and pre-industrial ozone and mercury, Atmos. Chem. Phys., 12, 6723-6740, 2012.
Parrington, M., Palmer, P. I., Henze, D. K., Tarasick, D. W., Hyer, E. J., Owen, R. C., Helmig, D., Clerbaux, C., Bowman, K. W., Deeter, M. N., Barratt, E. M., Coheur, P. F., Hurtmans, D., Jiang, Z., George, M., and Worden, J. R.: The influence of boreal biomass burning emissions on the distribution of tropospheric ozone over North America and the North Atlantic during 2010, Atmospheric Chemistry and Physics, 12, 2077-2098, 2012.
Parrington, M., Palmer, P. I., Lewis, A. C., Lee, J. D., Rickard, A. R., Di Carlo, P., Taylor, J. W., Hopkins, J. R., Punjabi, S., Oram, D. E., Forster, G., Aruffo, E., Moller, S. J., Bauguitte, S. J. B., Allan, J. D., Coe, H., and Leigh, R. J.: Ozone photochemistry in boreal biomass burning plumes, Atmospheric Chemistry and Physics, 13, 7321-7341, 2013.
Pfister, G. G., Emmons, L. K., Hess, P. G., Honrath, R., Lamarque, J. F., Martin, M. V., Owen, R. C., Avery, M. A., Browell, E. V., Holloway, J. S., Nedelec, P., Purvis, R., Ryerson, T. B., Sachse, G. W., and Schlager, H.: Ozone production from the 2004 North American boreal fires, Journal of Geophysical Research-Atmospheres, 111, 2006.
Pommier, M., Law, K. S., Clerbaux, C., Turquety, S., Hurtmans, D., Hadji-Lazaro, J., Coheur, P. F., Schlager, H., Ancellet, G., Paris, J. D., Nédélec, P., Diskin, G. S., Podolske, J. R., Holloway, J. S., and Bernath, P.: IASI carbon monoxide validation over the Arctic during POLARCAT spring and summer campaigns, Atmos. Chem. Phys., 10, 10655-10678, 2010.
Pugh, T. A. M., Cain, M., Methven, J., Wild, O., Arnold, S. R., Real, E., Law, K. S., Emmerson, K. M., Owen, S. M., Pyle, J. A., Hewitt, C. N., and MacKenzie, A. R.: A Lagrangian model of air-mass photochemistry and mixing using a trajectory ensemble: the Cambridge Tropospheric Trajectory model of Chemistry And Transport (CiTTyCAT) version 4.2, Geoscientific Model Development, 5, 193-221, 2012.
Quinn, P. K., Bates, T. S., Baum, E., Doubleday, N., Fiore, A. M., Flanner, M., Fridlind, A., Garrett, T. J., Koch, D., Menon, S., Shindell, D., Stohl, A., and Warren, S. G.: Short-lived pollutants in the Arctic:

their climate impact and possible mitigation strategies, Atmospheric Chemistry and Physics, 8, 1723-1735, 2008.
Real, E., Law, K. S., Weinzierl, B., Fiebig, M., Petzold, A., Wild, O., Methven, J., Arnold, S., Stohl, A., Huntrieser, H., Roiger, A., Schlager, H., Stewart, D., Avery, M., Sachse, G., Browell, E., Ferrare, R., and Blake, D.: Processes influencing ozone levels in Alaskan forest fire plumes during long-range transport over the North Atlantic, Journal of Geophysical Research-Atmospheres, 112, 2007.
Roiger, A., Schlager, H., Schafler, A., Huntrieser, H., Scheibe, M., Aufmhoff, H., Cooper, O. R., Sodemann, H., Stohl, A., Burkhart, J., Lazzara, M., Schiller, C., Law, K. S., and Arnold, F.: In-situ observation of Asian pollution transported into the Arctic lowermost stratosphere, Atmospheric Chemistry and Physics, 11, 10975-10994, 2011.
Shindell, D.: Local and remote contributions to Arctic warming, Geophysical Research Letters, 34, 2007.
Shindell, D. and Faluvegi, G.: Climate response to regional radiative forcing during the twentieth century, Nat. Geosci., 2, 294-300, 2009.
Shindell, D. T., Chin, M., Dentener, F., Doherty, R. M., Faluvegi, G., Fiore, A. M., Hess, P., Koch, D. M., MacKenzie, I. A., Sanderson, M. G., Schultz, M. G., Schulz, M., Stevenson, D. S., Teich, H., Textor, C., Wild, O., Bergmann, D. J., Bey, I., Bian, H., Cuvelier, C., Duncan, B. N., Folberth, G., Horowitz, L. W., Jonson, J., Kaminski, J. W., Marmer, E., Park, R., Pringle, K. J., Schroeder, S., Szopa, S., Takemura, T., Zeng, G., Keating, T. J., and Zuber, A.: A multi-model assessment of pollution transport to the Arctic, Atmospheric Chemistry and Physics, 8, 5353-5372, 2008.
Singh, H. B., Anderson, B. E., Brune, W. H., Cai, C., Cohen, R. C., Crawford, J. H., Cubison, M. J., Czech, E. P., Emmons, L., Fuelberg, H. E., Huey, G., Jacob, D. J., Jimenez, J. L., Kaduwela, A., Kondo, Y., Mao, J., Olson, J. R., Sachse, G. W., Vay, S. A., Weinheimer, A., Wennberg, P. O., Wisthaler, A., and Team, A. S.: Pollution influences on atmospheric composition and chemistry at high northern latitudes: Boreal and California forest fire emissions, Atmospheric Environment, 44, 4553-4564, 2010.
Singh, H. B. and Hanst, P. L.: PEROXYACETYL NITRATE (PAN) IN THE UNPOLLUTED ATMOSPHERE - AN IMPORTANT RESERVOIR FOR NITROGEN-OXIDES, Geophysical Research Letters, 8, 941-944, 1981.
Singh, H. B., O'Hara, D., Herlth, D., Bradshaw, J. D., Sandholm, S. T., Gregory, G. L., Sachse, G. W., Blake, D. R., Crutzen, P. J., and Kanakidou, M. A.: Atmospheric measurements of peroxyacetyl nitrate and other organic nitrates at high latitudes: Possible sources and sinks, Journal of Geophysical Research: Atmospheres, 97, 16511-16522, 1992.
Sodemann, H., Pommier, M., Arnold, S. R., Monks, S. A., Stebel, K., Burkhart, J. F., Hair, J. W., Diskin, G. S., Clerbaux, C., Coheur, P. F., Hurtmans, D., Schlager, H., Blechschmidt, A. M., Kristjansson, J. E., and Stohl, A.: Episodes of cross-polar transport in the Arctic troposphere during July 2008 as seen from models, satellite, and aircraft observations, Atmospheric Chemistry and Physics, 11, 3631-3651, 2011.
Tanimoto, H., Matsumoto, K., and Uematsu, M.: Ozone-CO Correlations in Siberian Wildfire Plumes Observed at Rishiri Island, Sola, 4, 65-68, 2008.
Thomas, J. L., Raut, J. C., Law, K. S., Marelle, L., Ancellet, G., Ravetta, F., Fast, J. D., Pfister, G., Emmons, L. K., Diskin, G. S., Weinheimer, A., Roiger, A., and Schlager, H.: Pollution transport from North America to Greenland during summer 2008, Atmospheric Chemistry and Physics, 13, 3825-3848, 2013.
van der Werf, G. R., Randerson, J. T., Giglio, L., Collatz, G. J., Mu, M., Kasibhatla, P. S., Morton, D. C., DeFries, R. S., Jin, Y., and van Leeuwen, T. T.: Global fire emissions and the contribution of deforestation, savanna, forest, agricultural, and peat fires (1997-2009), Atmospheric Chemistry and Physics, 10, 11707-11735, 2010.
Voulgarakis, A., Telford, P. J., Aghedo, A. M., Braesicke, P., Faluvegi, G., Abraham, N. L., Bowman, K. W., Pyle, J. A., and Shindell, D. T.: Global multi-year O3-CO correlation patterns from models and TES satellite observations, Atmos. Chem. Phys., 11, 5819-5838, doi:10.5194/acp-11-5819-2011, 2011.
Walker, T. W., Jones, D. B. A., Parrington, M., Henze, D. K., Murray, L. T., Bottenheim, J. W., Anlauf, K., Worden, J. R., Bowman, K. W., Shim, C., Singh, K., Kopacz, M., Tarasick, D. W., Davies, J., von der

Gathen, P., Thompson, A. M., and Carouge, C. C.: Impacts of midlatitude precursor emissions and local photochemistry on ozone abundances in the Arctic, Journal of Geophysical Research-Atmospheres, 117, 2012.
Warneke, C., Froyd, K. D., Brioude, J., Bahreini, R., Brock, C. A., Cozic, J., de Gouw, J. A., Fahey, D. W., Ferrare, R., Holloway, J. S., Middlebrook, A. M., Miller, L., Montzka, S., Schwarz, J. P., Sodemann, H., Spackman, J. R., and Stohl, A.: An important contribution to springtime Arctic aerosol from biomass burning in Russia, Geophysical Research Letters, 37, 2010.
Wespes, C., Emmons, L., Edwards, D. P., Hannigan, J., Hurtmans, D., Saunois, M., Coheur, P. F., Clerbaux, C., Coffey, M. T., Batchelor, R. L., Lindenmaier, R., Strong, K., Weinheimer, A. J., Nowak, J. B., Ryerson, T. B., Crounse, J. D., and Wennberg, P. O.: Analysis of ozone and nitric acid in spring and summer Arctic pollution using aircraft, ground-based, satellite observations and MOZART-4 model: source attribution and partitioning, Atmos. Chem. Phys., 12, 237-259, 2012.
Wofsy, S. C., Sachse, G. W., Gregory, G. L., Blake, D. R., Bradshaw, J. D., Sandholm, S. T., Singh, H. B., Barrick, J. A., Harriss, R. C., Talbot, R. W., Shipham, M. A., Browell, E. V., Jacob, D. J., and Logan, J. A.: ATMOSPHERIC CHEMISTRY IN THE ARCTIC AND SUB-ARCTIC - INFLUENCE OF NATURAL FIRES, INDUSTRIAL EMISSIONS, AND STRATOSPHERIC INPUTS, Journal of Geophysical Research-Atmospheres, 97, 16731-16746, 1992.

Zhang, B., Owen, R. C., Perlinger, J. A., Kumar, A., Wu, S., Val Martin, M., Kramer, L., Helmig, D., and Honrath, R. E.: A semi-Lagrangian view of ozone production tendency in North American outflow in the summers of 2009 and 2010, Atmos. Chem. Phys., 14, 2267-2287, doi:10.5194/acp-14-2267-2014, 2014.

906 **List of Tables**

907

Model	Resolution	Meteorology	Chemistry
CAM4-Chem	1.925° x 2.5°, 56 levels	GEOS-5	MOZART-4, bulk aerosols
CAM5-Chem	1.9° 25 x 2.5° 25 , 56 levels	GEOS-5	MOZART-4, modal aerosols
CIFS	1.125° 25 x 1.125° 25, 60 levels	ECMWF	tropospheric, CB05
GEOS-Chem	225° x 2.5° 25, 47 levels	GEOS-5	tropospheric, 100 species
GML	2° 25 x 2.5° 25, 72 levels	GEOS-5	stratospheric and tropospheric, 154 species, GOCART aerosols
LMDZ-INCA	1.925° x 3.75°25, 39 levels	ERA-Interim	tropospheric, 85 species, aerosols
MOZART-4	1.9° 25 x 2.5°, 56 levels	GEOS-5	tropospheric, 103 species, bulk aerosols
TM5	2° 25x 325°, 60 levels	ECMWF	tropospheric, CB05
TOMCAT	2.825° x 2.825°, 31 levels	ECMWF	tropospheric, 82 species
SMHI-MATCH	0.75° x 0.75°, 35 levels (hemispheric)	ECMWF	63 tracers, 110 gas-phase reactions Stratosphere: Monthly means from EU-MACC project (MOZART-4)

908

909 ***Table 1:*** *Description of POLMIP models.*

910

Steve 28/4/2015 08:36
Deleted: c

Steve 28/4/2015 08:36
Deleted: c

Steve 28/4/2015 08:47
Deleted: -

Steve 28/4/2015 08:41
Deleted: -GEOS5

	CAM4-Chem	CAM5-Chem	GMI	LMDZ-INCA	MOZART-4	TM5	TOMCAT
Longitude	202.5	200.0	182.5	228.8	172.5	169.5	205.3
Latitude	78.6	78.6	72.0	80.5	76.7	83.0	76.7
Pressure [hPa]	433.8	433.5	737.1	442.7	709.6	422.1	418.1
Ozone [ppbv]	57.8	61.7	62.0	64.8	43.7	53.6	75.6
CO [ppbv]	292.0	280.3	332.3	218.8	251.0	215.8	364.1
NO [pptv]	0.850	1.336	8.731	5.743	0.300	4.974	6.281
NO_2 [pptv]	0.663	1.079	32.473	7.612	5.721	2.618	7.815
$HONO_2$ [pptv]	4.912	0.757	784.2	288.3	0.093	2.580	463.9
PAN [pptv]	182.7	207.3	93.86	407.1	97.41	448.6	1476.
H_2O_2 [ppbv]	1.115	1.719	3.492	0.000	1.235	0.000	2.120
MeOOH [ppbv]	0.425	0.579	1.034	0.000	0.836	0.476	0.000
C_2H_6 [ppbv]	2.165	2.067	2.451	1.642	1.779	1.653	2.637
C_3H_8 [ppbv]	0.128	0.083	0.130	0.078	0.101	0.082	0.110
Acetone [ppbv]	1.456	1.417	0.000	0.746	1.185	0.345	1.445
Acetaldehyde [ppbv]	0.051	0.046	0.069	0.022	0.126	0.015	0.054
OH [10^6 molec cm^{-3}]	0.42	0.65	1.07	0.45	0.05	0.46	0.48

915

916 ***Table 2:*** *Positions and chemical composition of fire plume maxima in the POLMIP model simulations at 06 UT*
917 *on 7th July 2008. Plume maxima positions are defined based on abundance of simulated 25-day fixed-lifetime*
918 *Asian biomass burning tracer. See text for details.*

919

920

Steve 28/4/2015 08:36
Deleted: c

Steve 28/4/2015 08:37
Deleted: c

Steve 28/4/2015 12:56
Deleted: 197.5

Steve 28/4/2015 12:57
Deleted: 6.7

Steve 28/4/2015 12:57
Deleted: 71

Steve 28/4/2015 12:57
Deleted: 5

Steve 28/4/2015 12:57
Deleted: 7

Steve 28/4/2015 13:35
Formatted Table

Steve 28/4/2015 13:35
Formatted: Superscript

Steve 28/4/2015 13:35
Formatted: Superscript

List of Figures

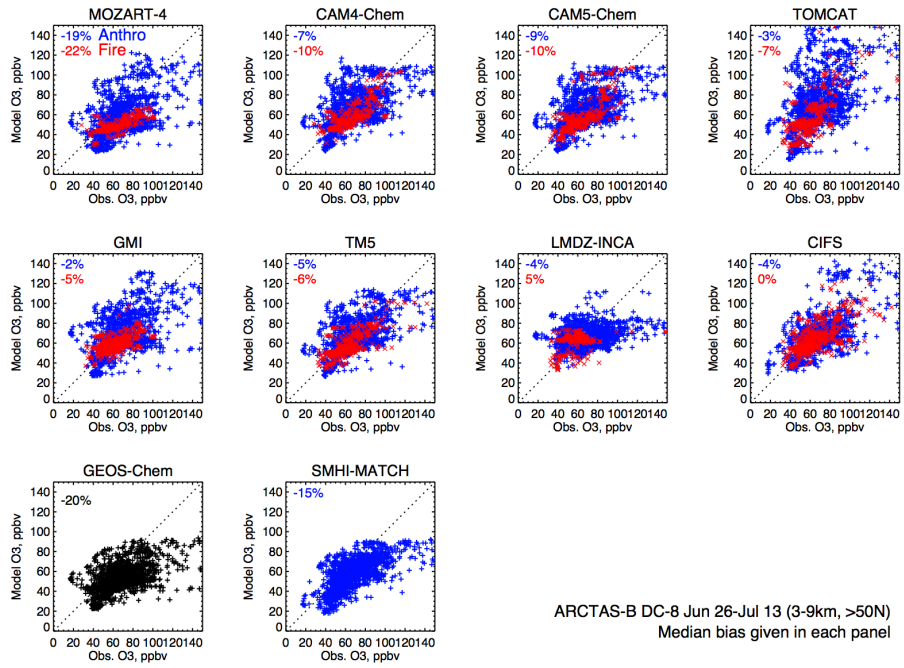

Figure 1: *POLMIP model ozone interpolated to selected ARCTAS-B DC8 flight tracks north of 50N, and between3-9km altitude plotted as a function of the DC8-observed concentrations. Blue and red colours show model points which are dominated by anthropogenic and biomass burning emissions respectively, as diagnosed by 25-day fixed-lifetime CO tracers simulated by the models (see text for details). Mean fractional model biases (%) in anthropogenic- and fire-dominated air are shown in blue and red text respectively. The GEOS-Chem model did not simulate 25-day fixed lifetime tracers.*

Unknown
Formatted: Font:12 pt, Bold

Steve 28/4/2015 08:33
Deleted: *c*

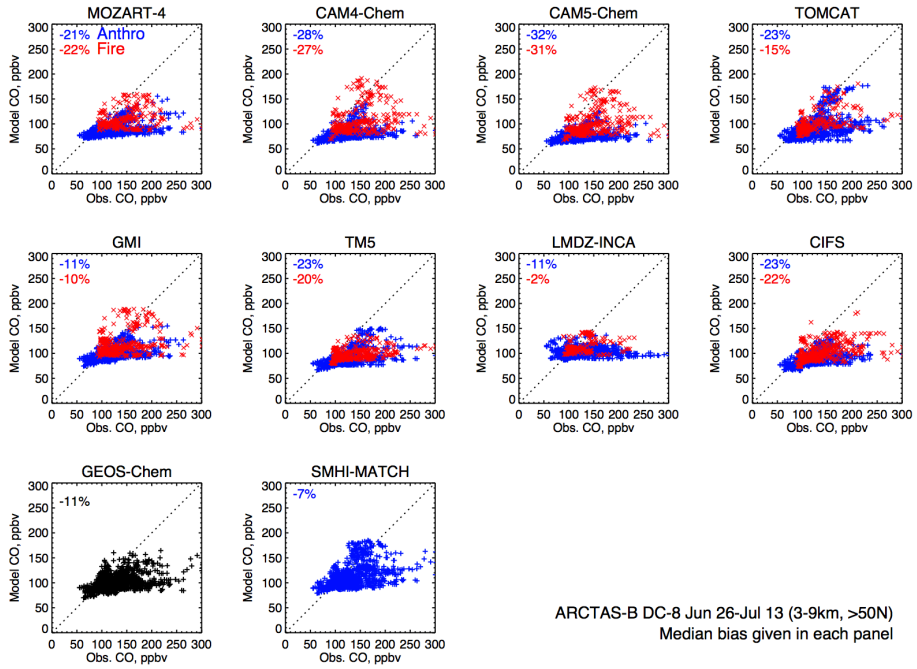

938

939 ***Figure 2**: As Fig 1., but for CO.*

Unknown

Formatted: Font:12 pt, Bold

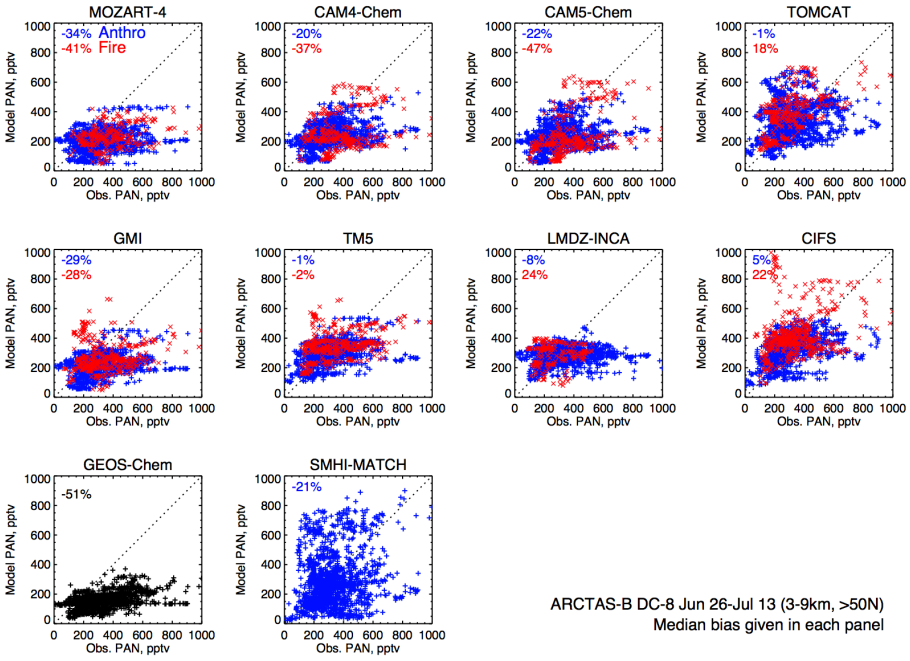

940

941 ***Figure 3***: *As Fig 1., but for PAN.*

Unknown

Formatted: Font:Bold

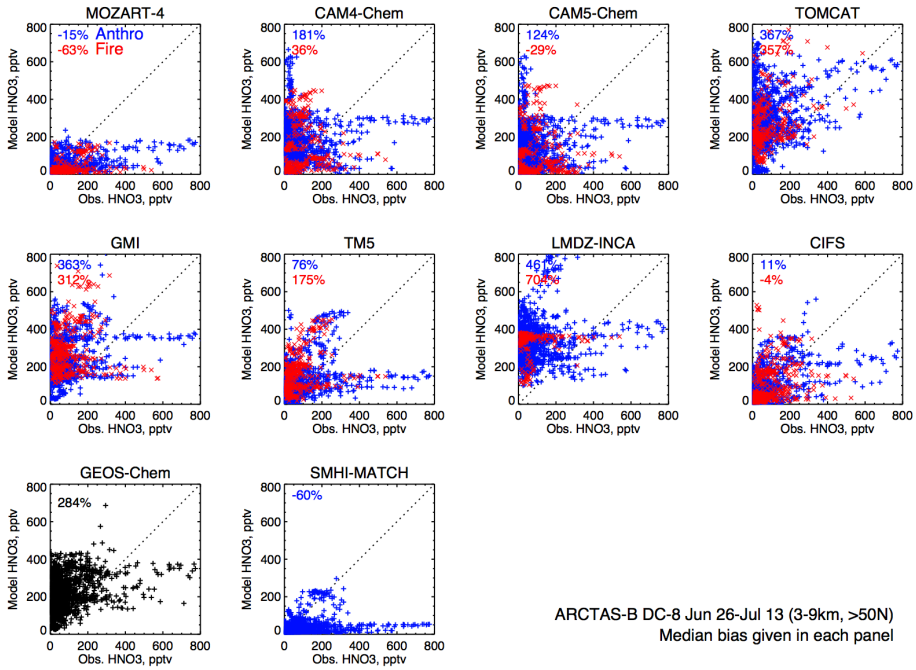

942

943 ***Figure 4***: *As Fig 1., but for HNO_3.*

Unknown

Formatted: Font:Bold

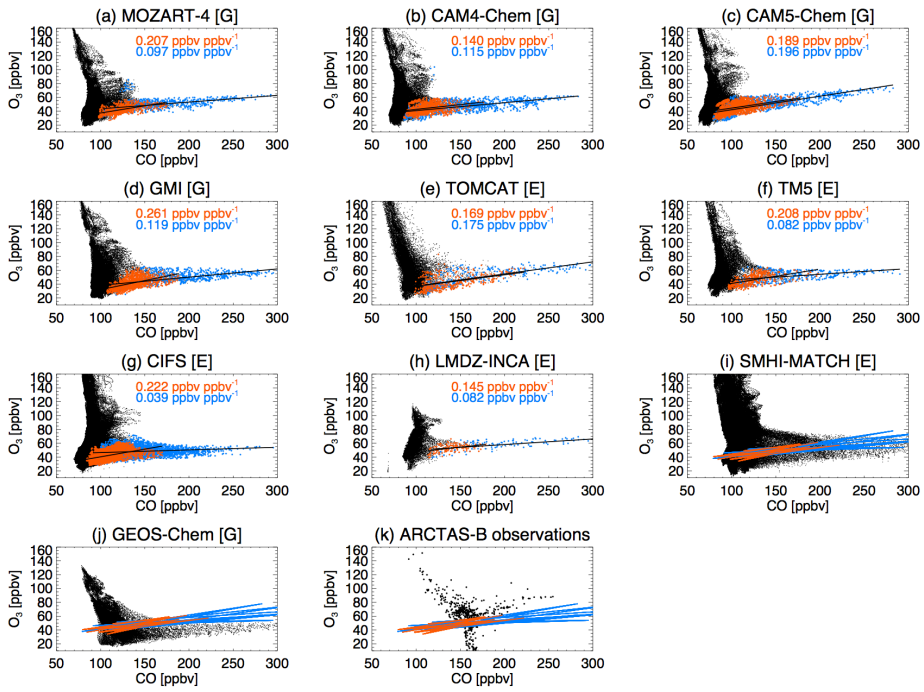

944

945 ***Figure 5***: *July 2008 monthly-mean O_3 vs CO from POLMIP model simulations coloured by fire*
946 *influence and relative age of air since emission. Black: all points north of 50N, with 850 hPa >*
947 *pressure > 250 hPa. Coloured points show model grid boxes where the fire-emitted fixed-lifetime CO*
948 *tracer contributes more than 66% of the total (fire + anthropogenic) tracer mixing ratio. Blue and red*
949 *points denote younger than average and more aged than average of these points respectively, as*
950 *diagnosed by the ln([C3H8]/[C2H6]) concentration ratio. Models that did not simulate fixed-lifetime*
951 *tracers, or do not carry [C3H8] explicitly, do not have coloured points, but instead show slopes from*
952 *linear regressions of the coloured points from the other models (red and blue lines). Red and blue text*
953 *give $\Delta O_3/\Delta CO$ slope values from linear regressions of the youngest and most aged populations*
954 *respectively. Letters in square brackets denote the meteorological analysis data used to drive the*
955 *models - E: ECMWF; G: GEOS-5. Panel (k) shows ARCTAS-B aircraft observations.*

Steve 28/4/2015 11:21
Deleted: *Red*

Steve 28/4/2015 11:22
Deleted: *blue*

Steve 28/4/2015 11:14
Deleted: *st*

Steve 28/4/2015 11:14
Deleted: *most*

Steve 28/4/2015 11:14
Deleted: *50%*

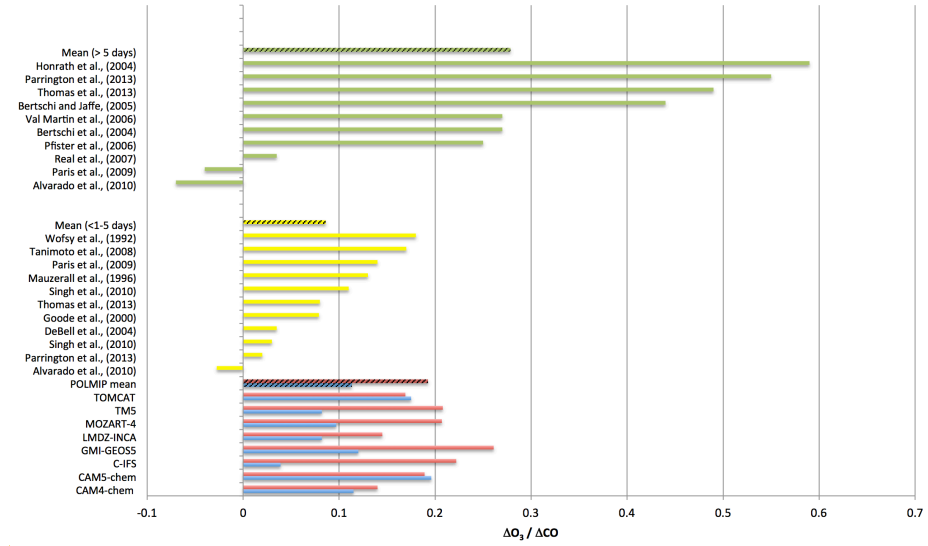

Figure 6**:** *$\Delta O_3/\Delta CO$ ratios in boreal biomass burning pollution from previous studies and from the POLMIP model simulations analysed in this study. Green: values from plumes of age > 5 days; yellow: values from plumes of age <1-5 days. POLMIP model values are classified by age since emission (red: aged; blue: young), based on the by the $\ln([C_3H_8]/[C_2H_6])$ concentration ratio (see text for details). Hatched bars indicate average values for each category. Literature values for previous studies are based on an updated version of the review of Jaffe and Wigder, (2012).*

Unknown
Formatted: Font:10 pt

Steve 29/4/2015 09:13
Formatted: Subscript

Steve 29/4/2015 09:13
Formatted: Subscript

Steve 29/4/2015 09:13
Formatted: Subscript

Steve 29/4/2015 09:13
Formatted: Subscript

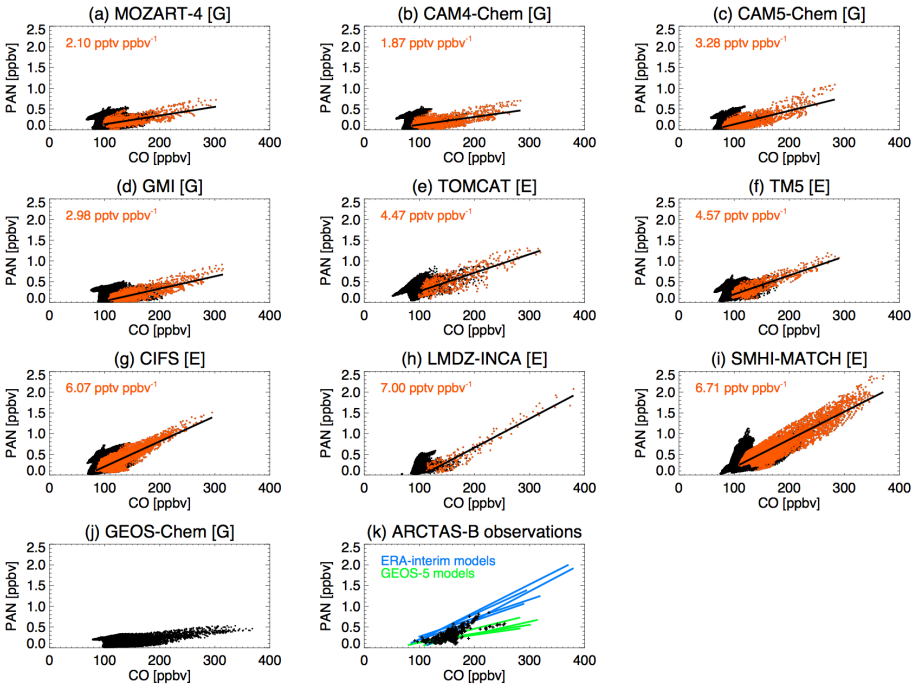

Figure 7: *July 2008 PAN/CO relationships for POLMIP models coloured by fire influence. Black: all points north of 50N, with 850 hPa > pressure > 250 hPa. Red points show model grid boxes where the fire fixed-lifetime CO tracer contributes more than 66% of the total (fire + anthropogenic) tracer mixing ratio. Red text gives ΔPAN/ΔCO slope values for linear regressions of the red points. GEOS-Chem model did not supply fixed-lifetime tracers. Letters in square brackets denote the meteorological analysis data used to drive the models - E: ECMWF; G: GEOS-5. Panel (k) shows ARCTAS-B aircraft observations with slopes from ECMWF (blue) and GEOS-5 (green) models shown for comparison.*

Unknown

Formatted: Font:Italic

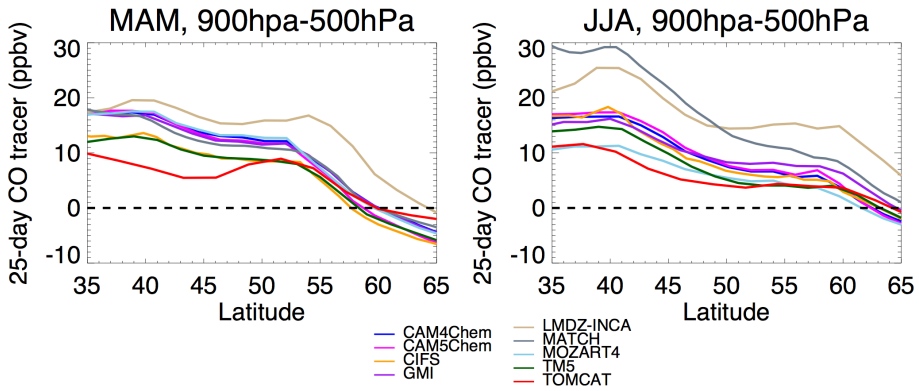

977

978 ***Figure 8:*** *Zonally-averaged difference between simulated 25-day fixed lifetime CO tracer mixing*
979 *ratios at 900 hPa and 500 hPa in the POLMIP model simulations for (a) spring (MAM) and (b) summer*
980 *(JJA) 2008.*

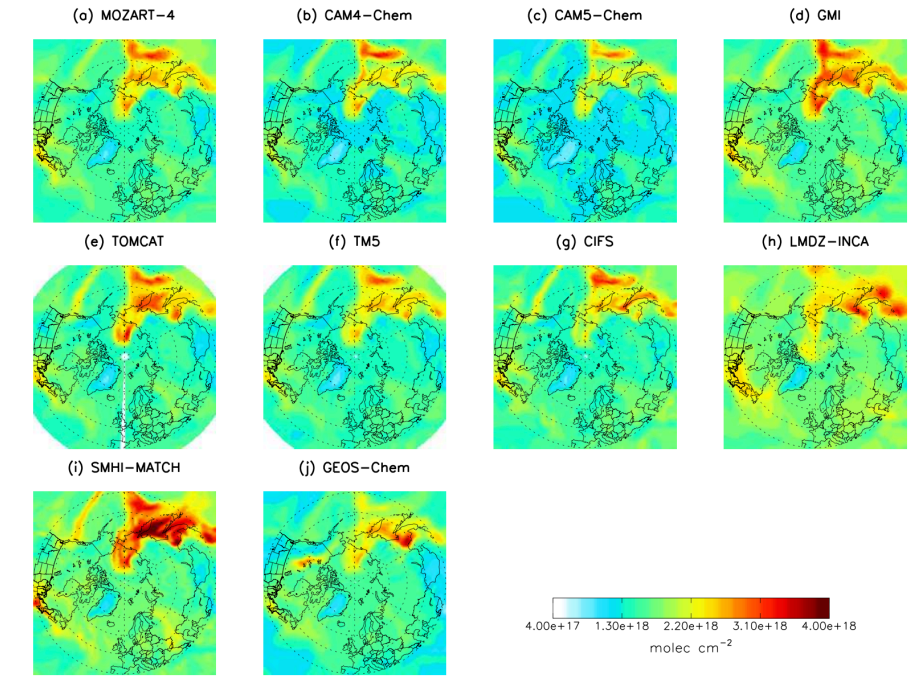

981

982 ***Figure 9:*** *Total column CO from the POLMIP model simulations at 06UT on 7th July 2008.*

983

Unknown
Formatted: Font:Bold, Italic

Unknown
Formatted: Font:Bold, Italic

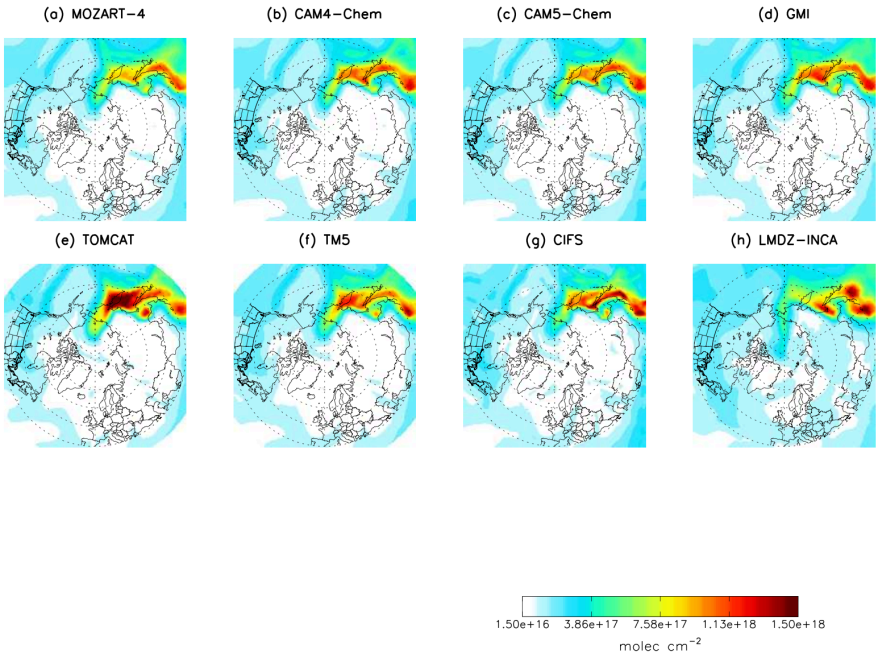

Unknown
Formatted: Font:Bold, Italic

Figure 10: *Total column concentrations of the 25-day fixed-lifetime Asian anthropogenic tracer from the POLMIP model simulations at 06UT on 7th July 2008.*

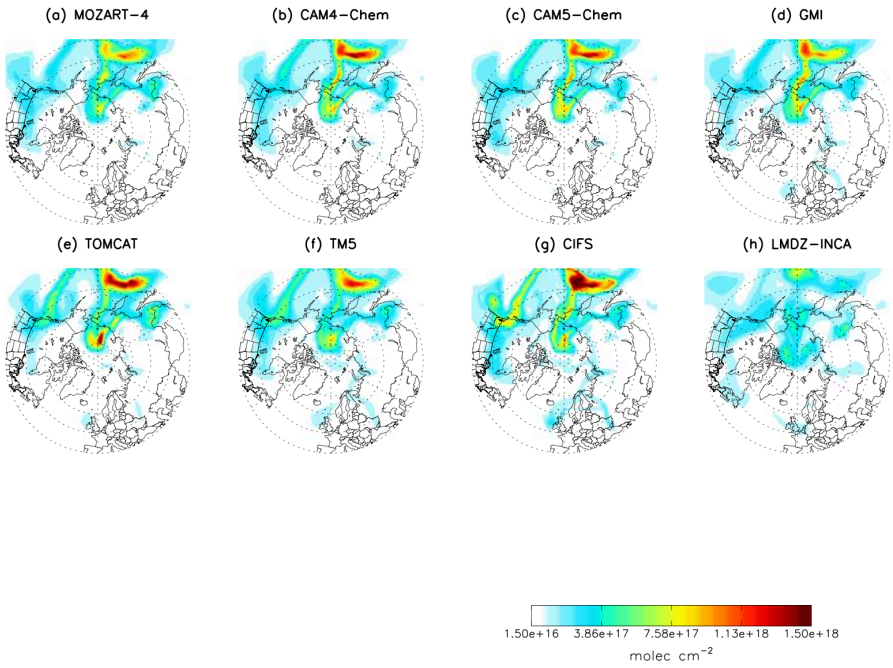

Unknown
Formatted: Font:Italic

Figure 11: *Total column concentrations of the 25-day fixed-lifetime Asian fire tracer from the POLMIP model simulations at 06UT on 7th July 2008.*

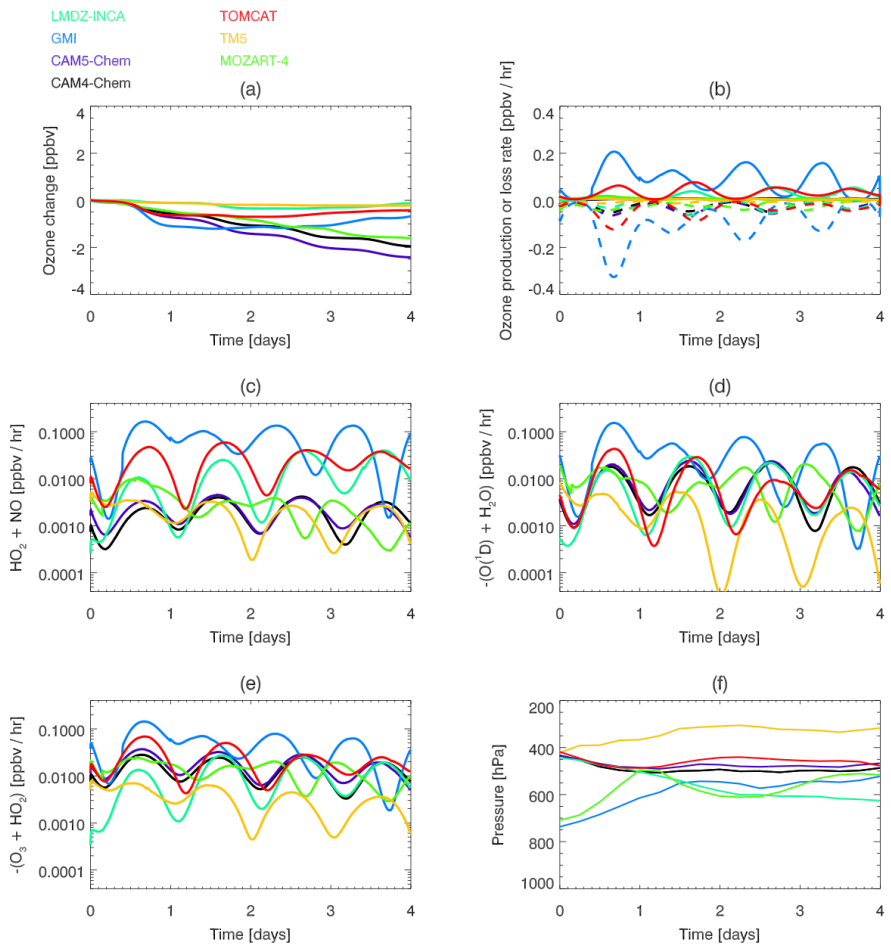

991

992 ***Figure 12:*** *CiTTyCAT Lagrangian box model simulations of fire plume ozone evolution in the Arctic.*
993 *Coloured lines show simulations initialised with chemical composition from each of the POLMIP*
994 *global models at the fire plume maxima locations at 06UT on 7th July 2008. (a) Net ozone change*
995 *over the 4-day simulations. (b) Integrated ozone production (solid) and loss (dashed) rates. (c) Rate of*
996 *HO_2+NO ozone production; (d) Rate of $O(^1D) + H_2O$ ozone loss; (e) Rate of $HO_2 + O_3$ ozone loss; (f)*
997 *Pressure of forward trajectories from each POLMIP model plume maximum position used for the*
998 *Lagrangian simulations. See text for details of the Lagrangian model simulations.*

999

1000

Unknown
Formatted: Font:Italic

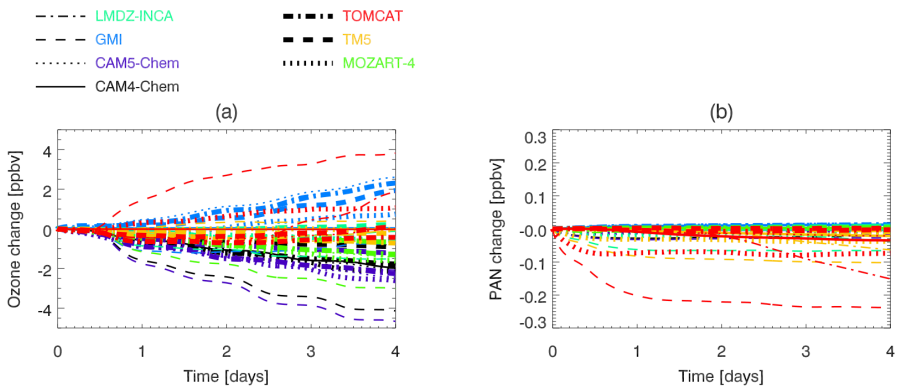

Unknown
Formatted: Font:Bold, Italic

Figure 13: *Time evolution of fire plume ozone (a) and PAN (b) from CiTTyCAT Lagrangian model simulations in which the initial plume concentrations from each of the POLMIP models have been used in combination with each of the forward trajectories from the different POLMIP model plume positions (shown in Fig. 12f). Different colours correspond to the POLMIP model initial chemical conditions and line styles correspond to POLMIP model forward trajectories.*

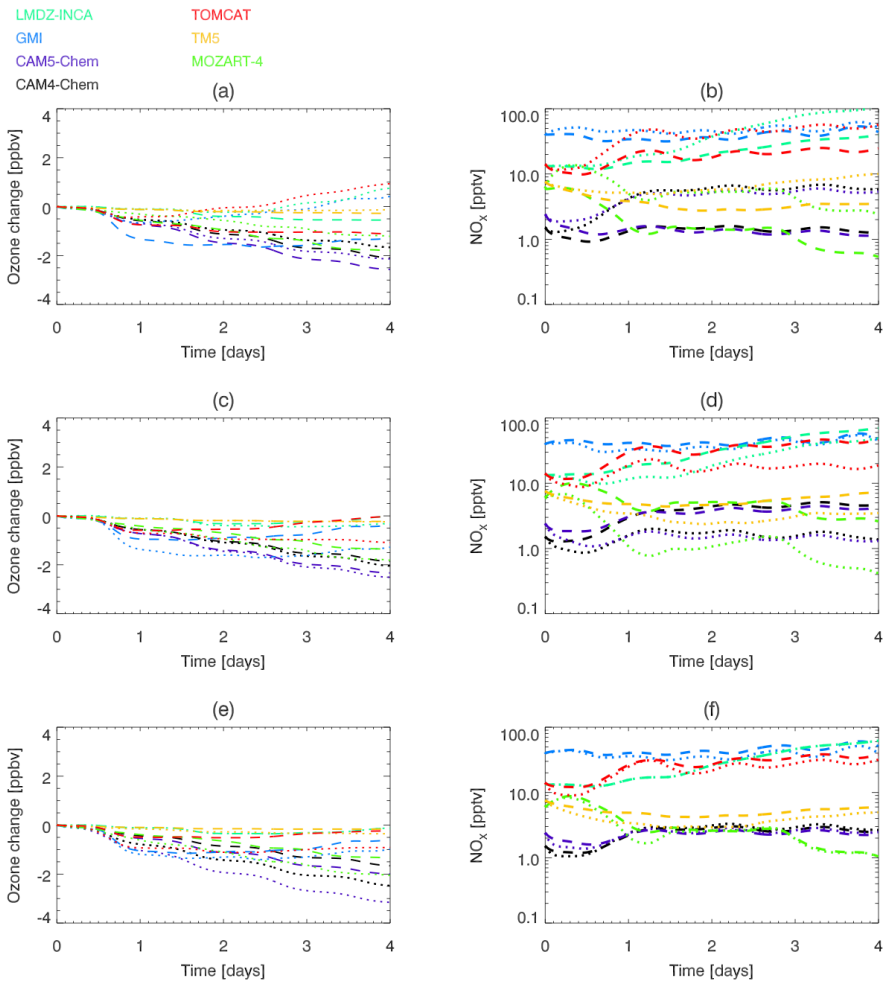

Unknown

Formatted: Font:Bold, Italic

Figure 14: *CiTTyCAT Lagrangian box model simulations showing sensitivity of fire plume ozone and NO_X evolution in the Arctic to initial concentrations of key species. Dotted and dashed lines show simulations initiailsed with 200% and 50% respectively of PAN (a-b), acetone and acetaldehyde (c-d), H_2O_2 and CH_3OOH (e-f). Ozone change from simulations with un-perturbed initial concentrations are shown in Fig. 12a.*